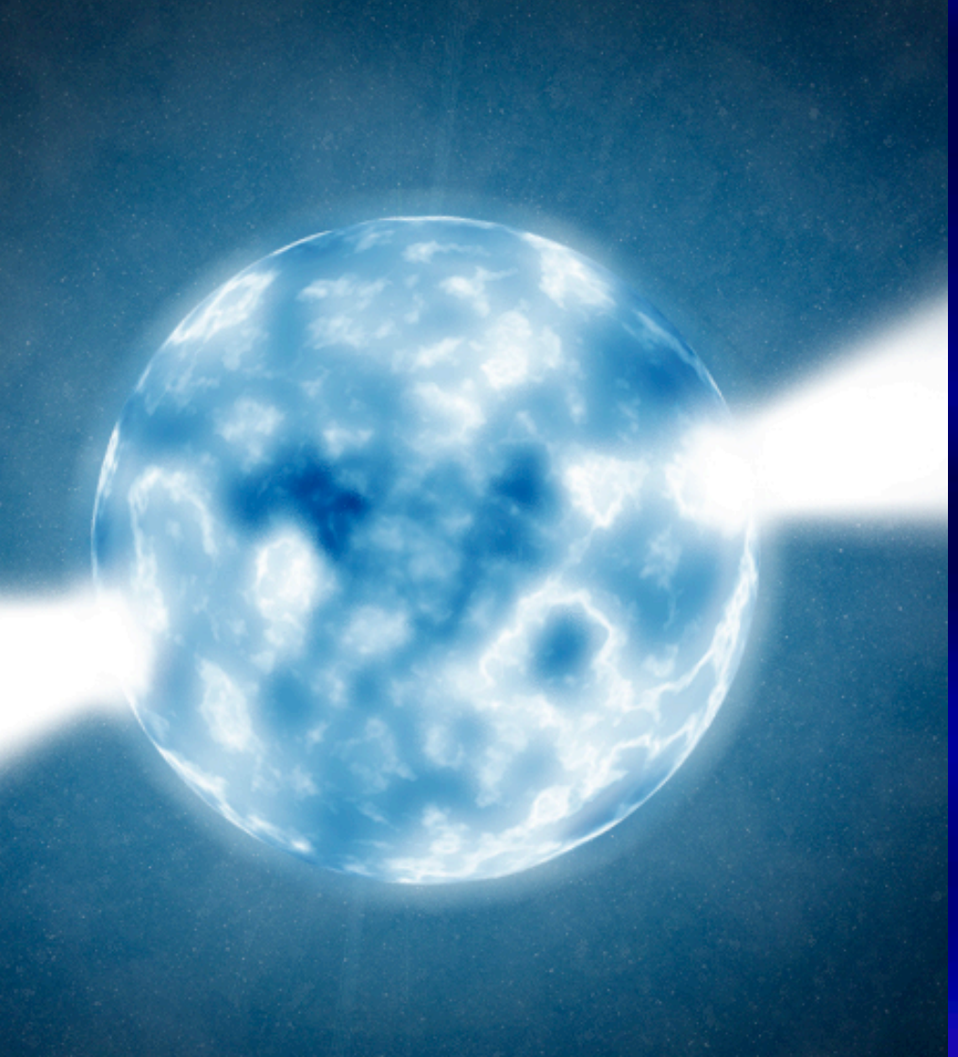

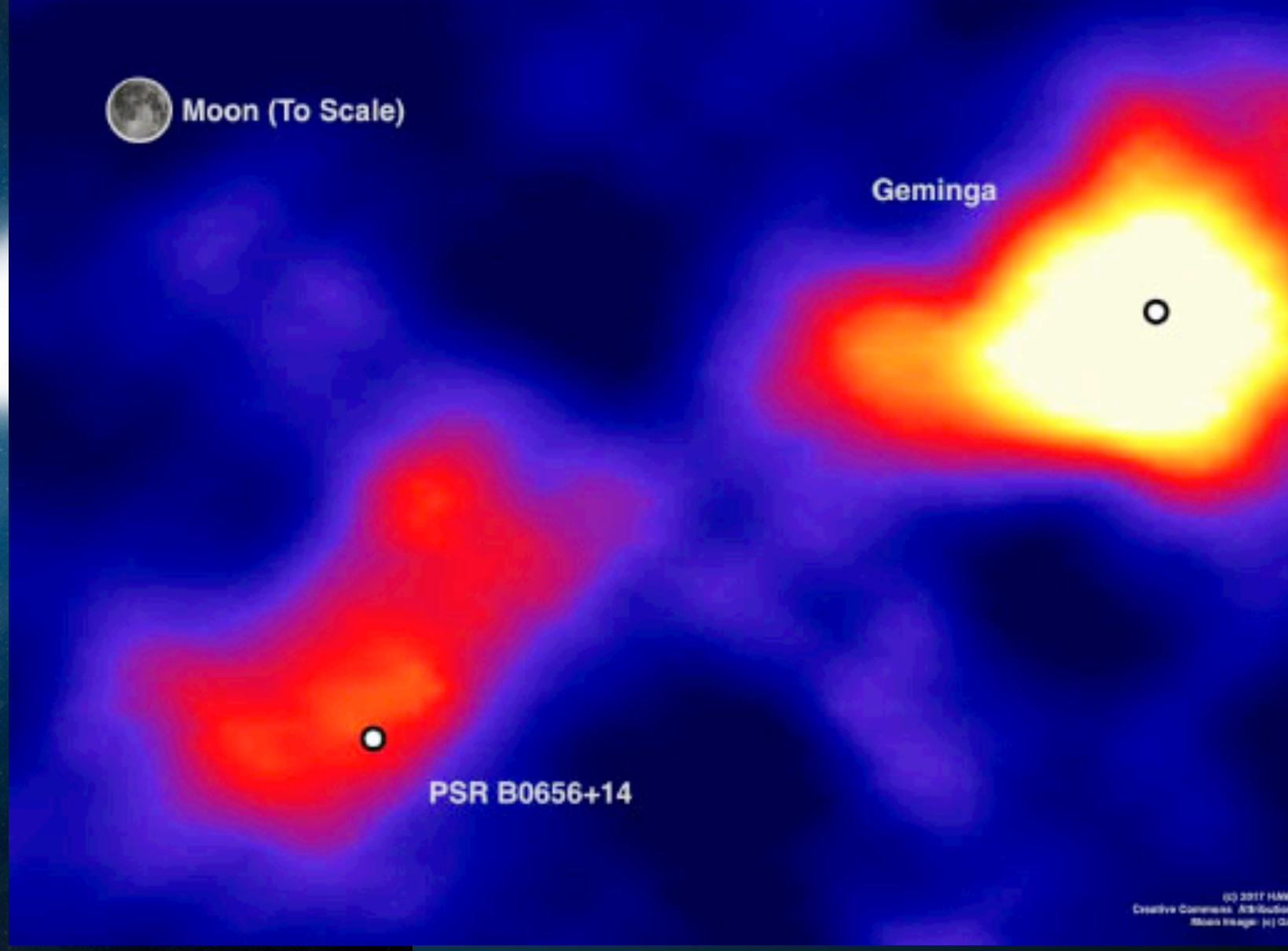

TIM LINDEN

TEV HALO OBSERVATIONS WITH HAWC

HAWC Weekly Meeting

THE OHIO STATE UNIVERSITY
CENTER FOR COSMOLOGY AND ASTROPARTICLE PHYSICS

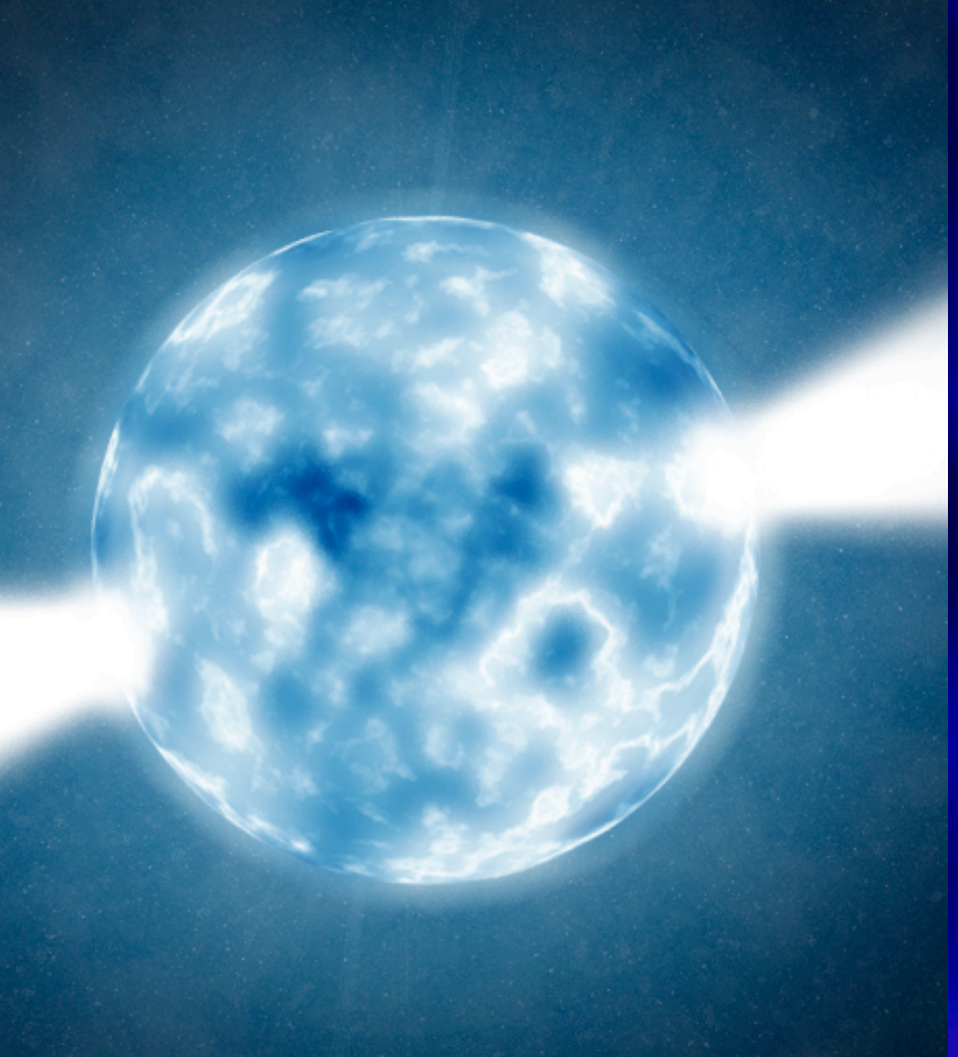

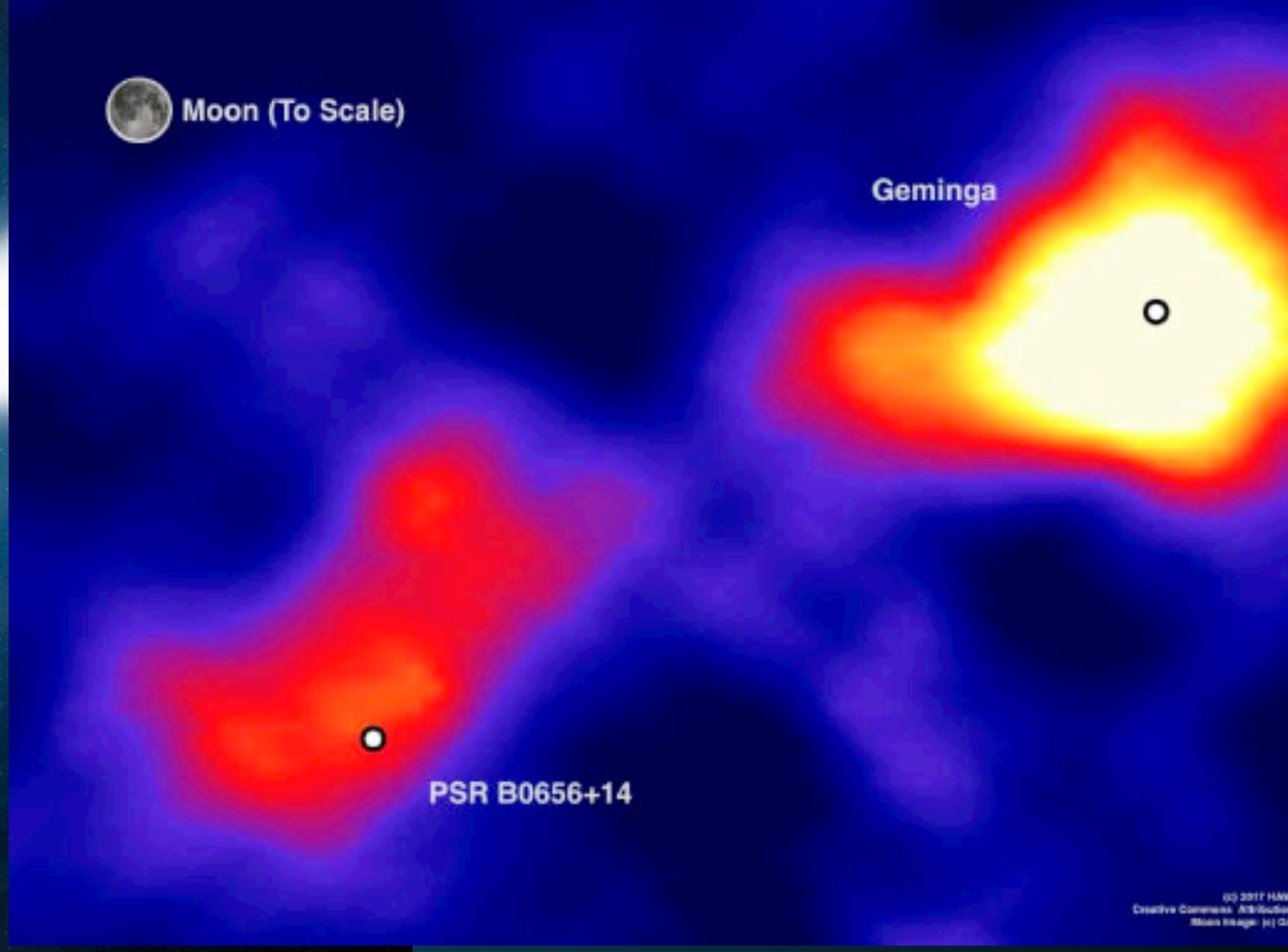

TIM LINDEN

WITH: KATIE AUCHETTL, BEN BUCKMAN, JOSEPH BRAMANTE, ILIAS CHOLIS, CARMELO EVOLI, KE FANG, DAN HOOPER, TANVI KARWAL, SHIRLEY LI, GIOVANNI MORLINO

HAWC Weekly Meeting

THE OHIO STATE UNIVERSITY
CENTER FOR COSMOLOGY AND ASTROPARTICLE PHYSICS

CONCLUSIONS

- TeV halos are a new dynamical object.

- TeV halos should produce the majority of both point-source and diffuse emission observed by HAWC.

- HAWC is particularly well-suited for TeV halo observations.

- Multiple questions remain unanswered:
  - How are TeV halos formed?
  - Do all pulsars produce TeV halos? Environmental Effects?
  - Do MSPs produce TeV halos?

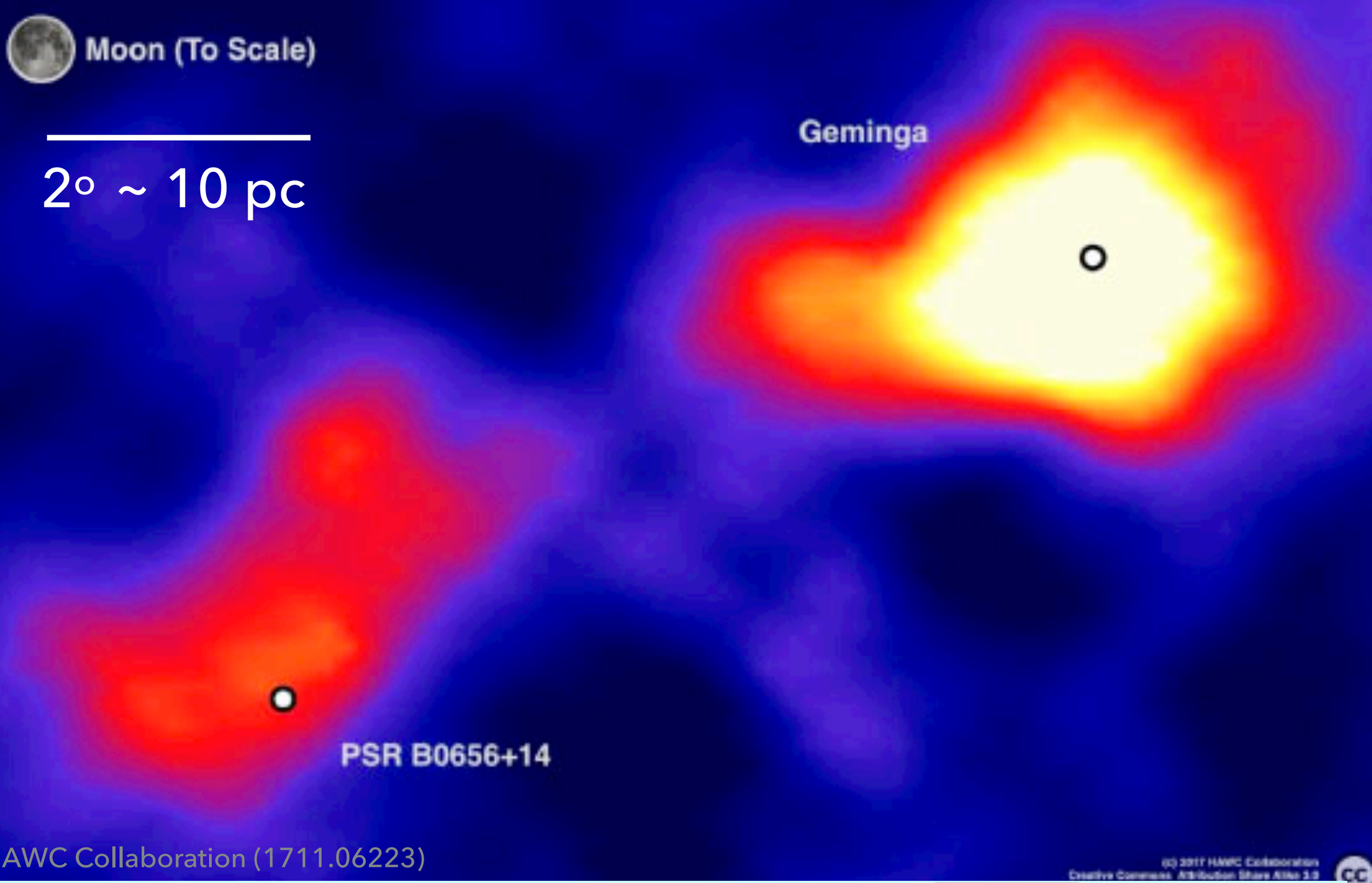

#	NAME		RAJD (deg)	DECJD (deg)	DIST (kpc)	AGE (Yr)	EDOT (ergs/s)	C1
1	J0633+1746	hh92	98.47564	17.77025	0.19	3.42e+05	3.2e+34	7.0540e+34
2	B0656+14	mlt+78	104.95056	14.23931	0.29	1.11e+05	3.8e+34	3.5957e+34

HAWC Collaboration (1711.06223)

2°

Geminga

Pulsar Parameters		Geminga	PSR B0656+14
(Right ascension, declination) (J2000 source location)	[degrees]	(98.48, 17.77)	(104.95, 14.24)
τ_c (characteristic age)	[years]	342,000	110,000
T (spin period)	[seconds]	0.237	0.385
d (distance)	[parsecs]	250^{+120}_{-62}	288^{+33}_{-27}
dE/dt (energy loss rate due to pulsar's spin slowing)	[x10^{34} ergs/sec]	3.26	3.8
Model Values			
θ_0 (θ_d for 20 TeV γ-ray)	[degrees]	5.5 ± 0.7	4.8 ± 0.6
N_0	[x10^{-15} photons/TeV/cm^2 /sec]	$13.6^{+2.0}_{-1.7}$	$5.6^{+2.5}_{-1.7}$
α		2.34 ± 0.07	2.14 ± 0.23
D_{100} (Diffusion coefficient of 100TeV electrons from joint fit of two PWNe)	[x10^{27} cm^2/sec]	4.5 ± 1.2	4.5 ± 1.2
D_{100}(Diffusion coefficient of 100TeV electrons from individual fit of PWN)	[x10^{27} cm^2/sec]	$3.2^{+1.4}_{-1.0}$	15^{+49}_{-9}
Energy Range	[TeV]	8 to 40	8 to 40
Luminosity in gamma-rays over this energy range	[x10^{31} erg/sec]	11x(d/250 parsec)^2	4.5x(d/288 parsec)^2
Assumed Parameters			
L_0 (initial spin down power)	[x10^{36} ergs/sec]	27.8	4.0
W_e (total energy released since pulsar's birth)	[x10^{48} ergs]	11.0	1.5

Table 1: Pulsar parameters, values of parameters from the model fitting to the observed extended gamma-ray emission, and assumed parameters of our model. Pulsar parameters are from (14).

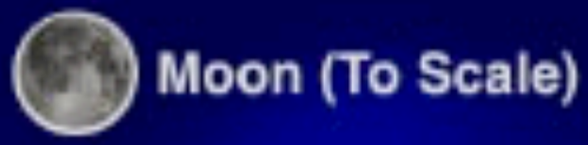

2° ~ 10 pc

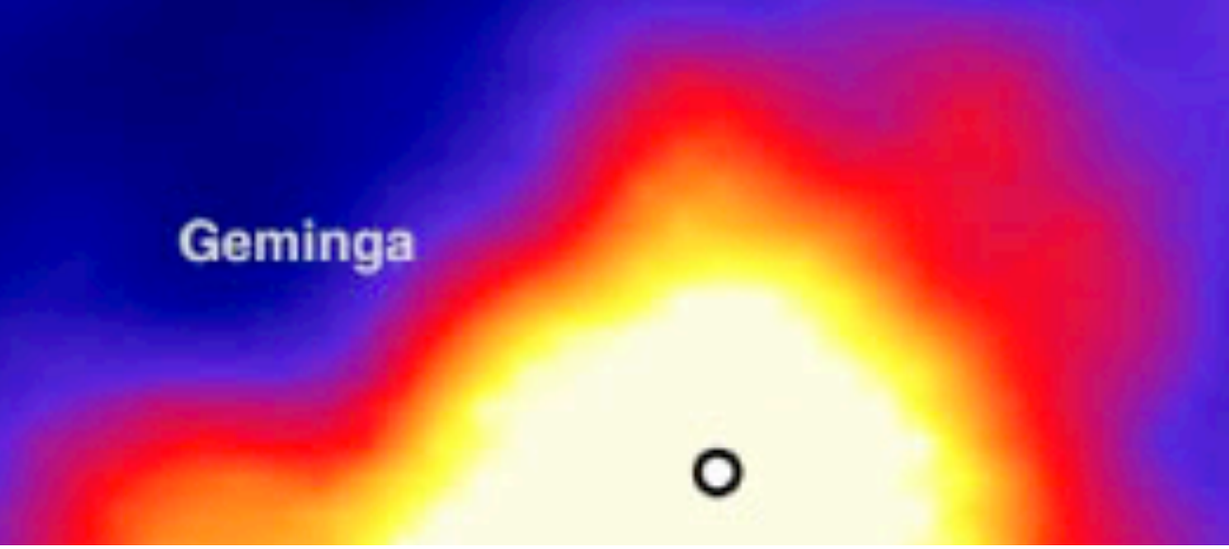

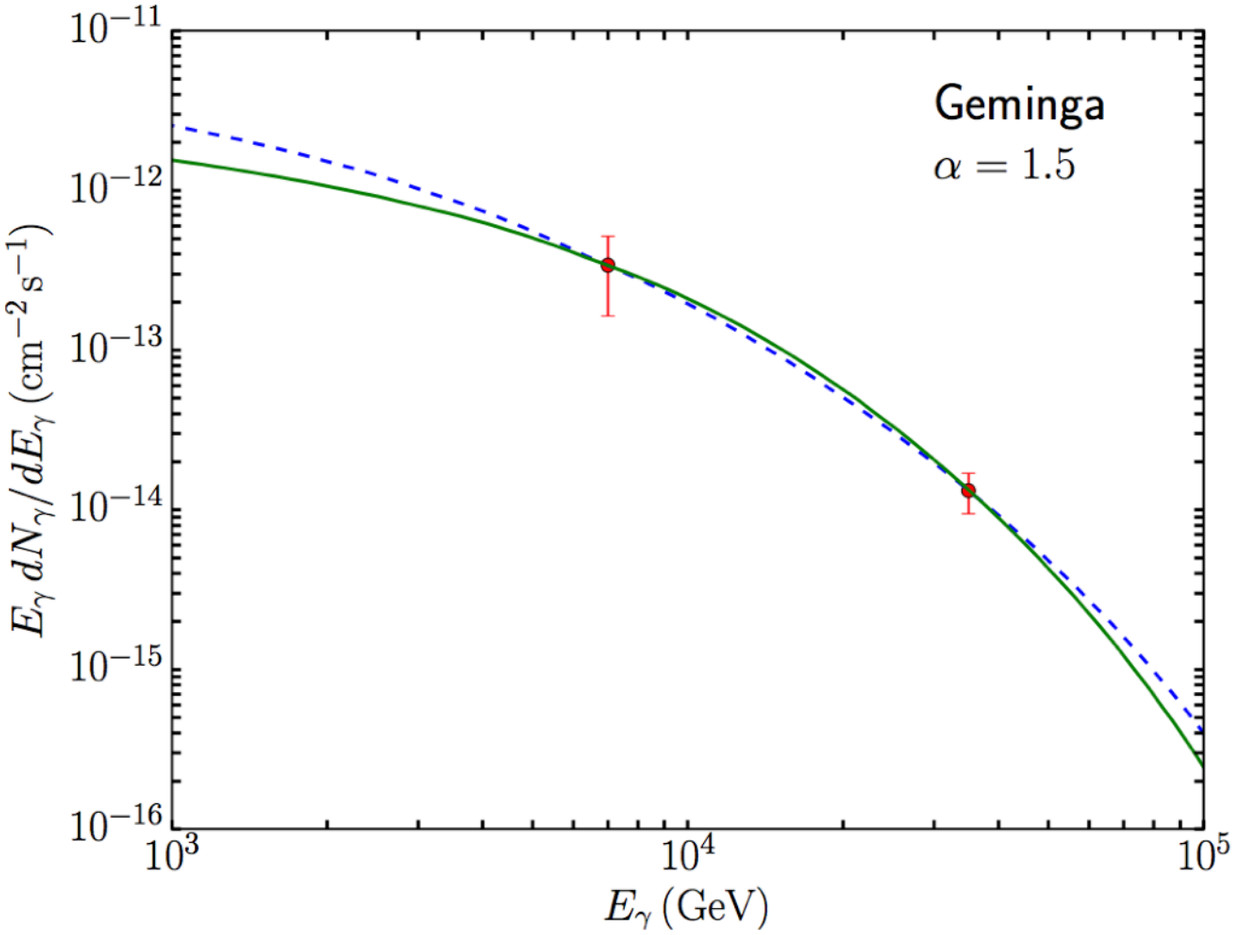

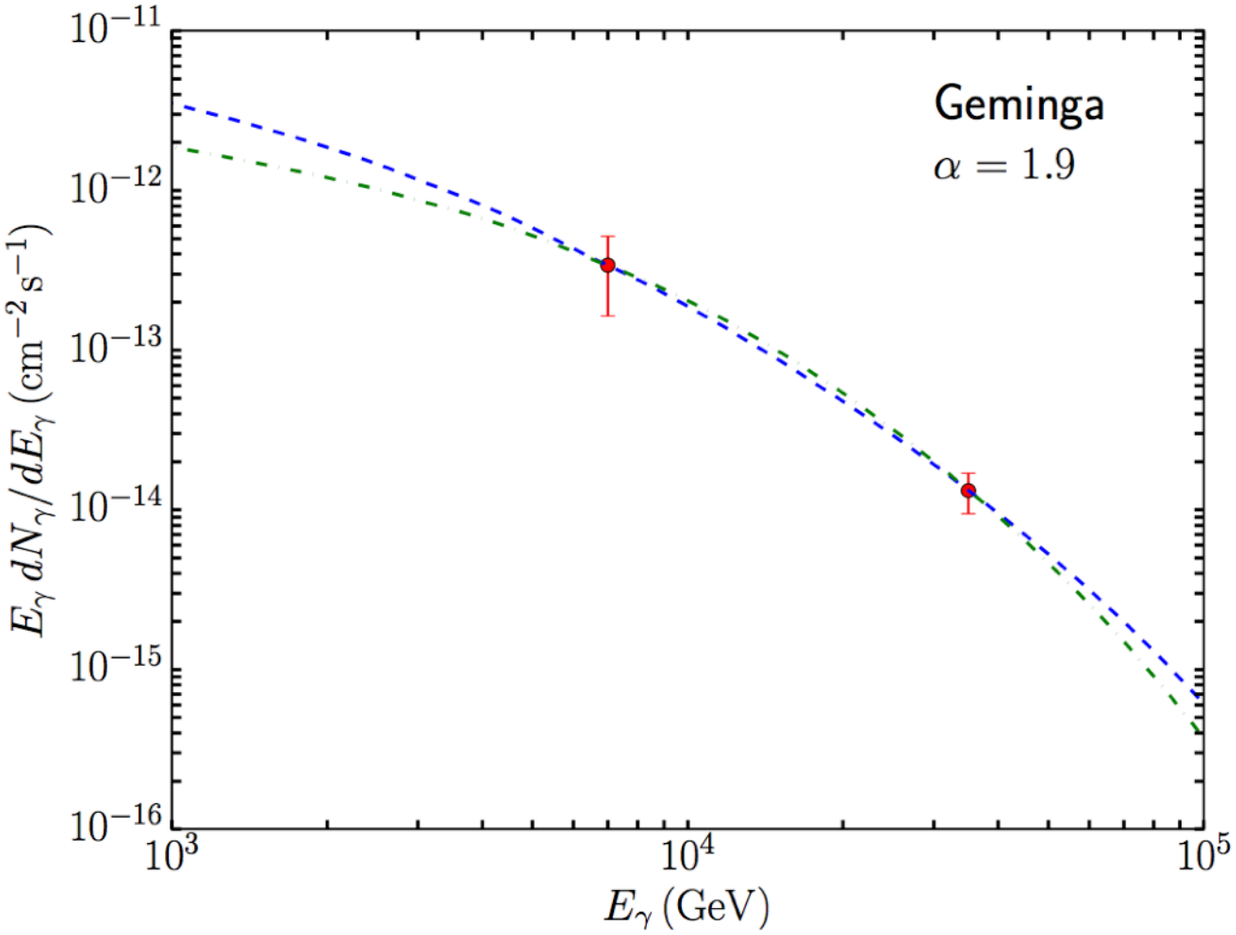

Hooper et al. (1702.08436)

Conversion to the e^+e^- population, and then an extrapolation to 1 GeV indicates that more than 10% of the spin down energy is converted into e^+e^- pairs.

TEV HALOS

HAWC Collaboration (Nature; 1711.06223)

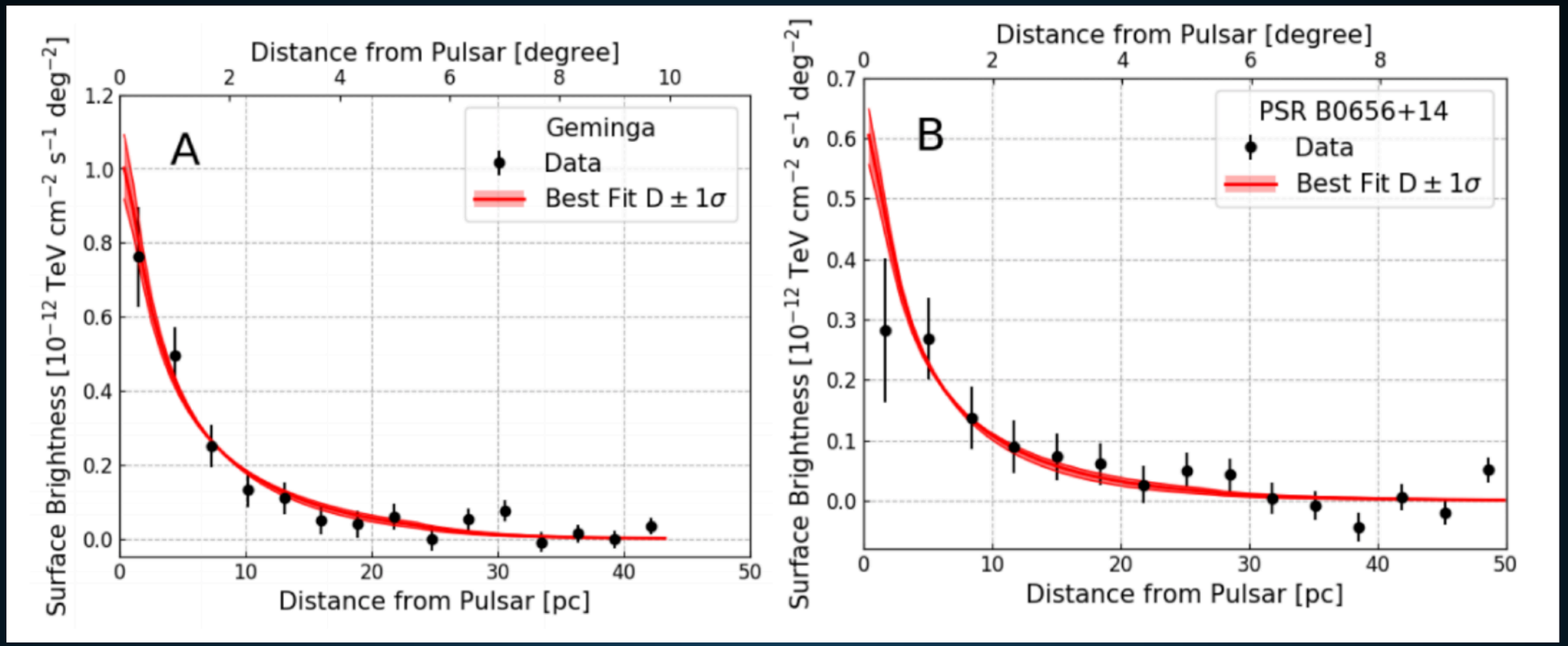

- **Why TeV Halos?**
  - **These sources are <u>much larger</u> than PWN**

$$R_{\rm PWN} \simeq 1.5 \left(\frac{\dot{E}}{10^{35}\,{\rm erg/s}}\right)^{1/2} \times \left(\frac{n_{\rm gas}}{1\,{\rm cm}^{-3}}\right)^{-1/2} \left(\frac{v}{100\,{\rm km/s}}\right)^{-3/2} {\rm pc}$$

TEV HALOS

Posselt et al. (1611.03496)

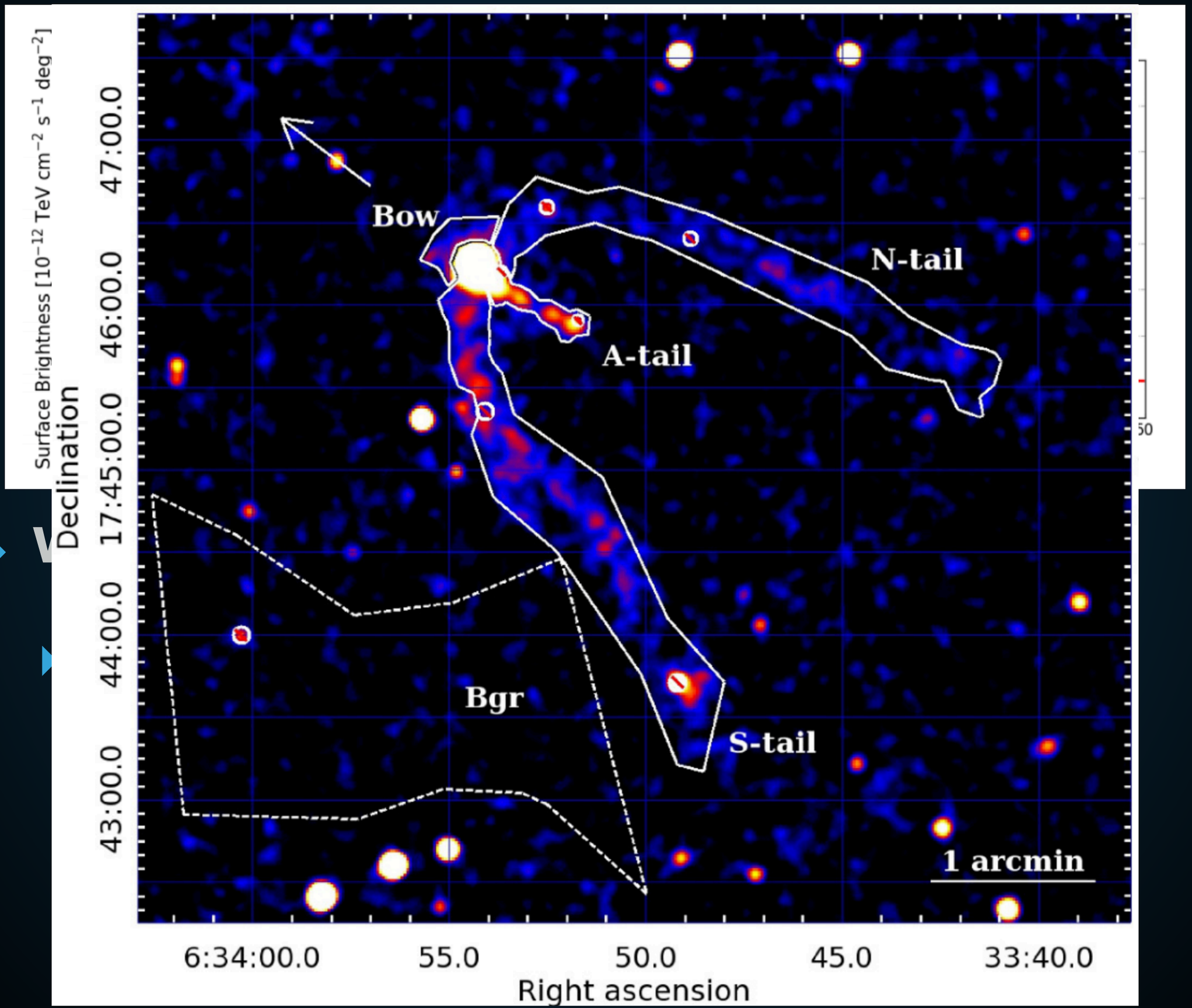

TEV HALOS

HAWC Collaboration (Nature; 1711.06223)

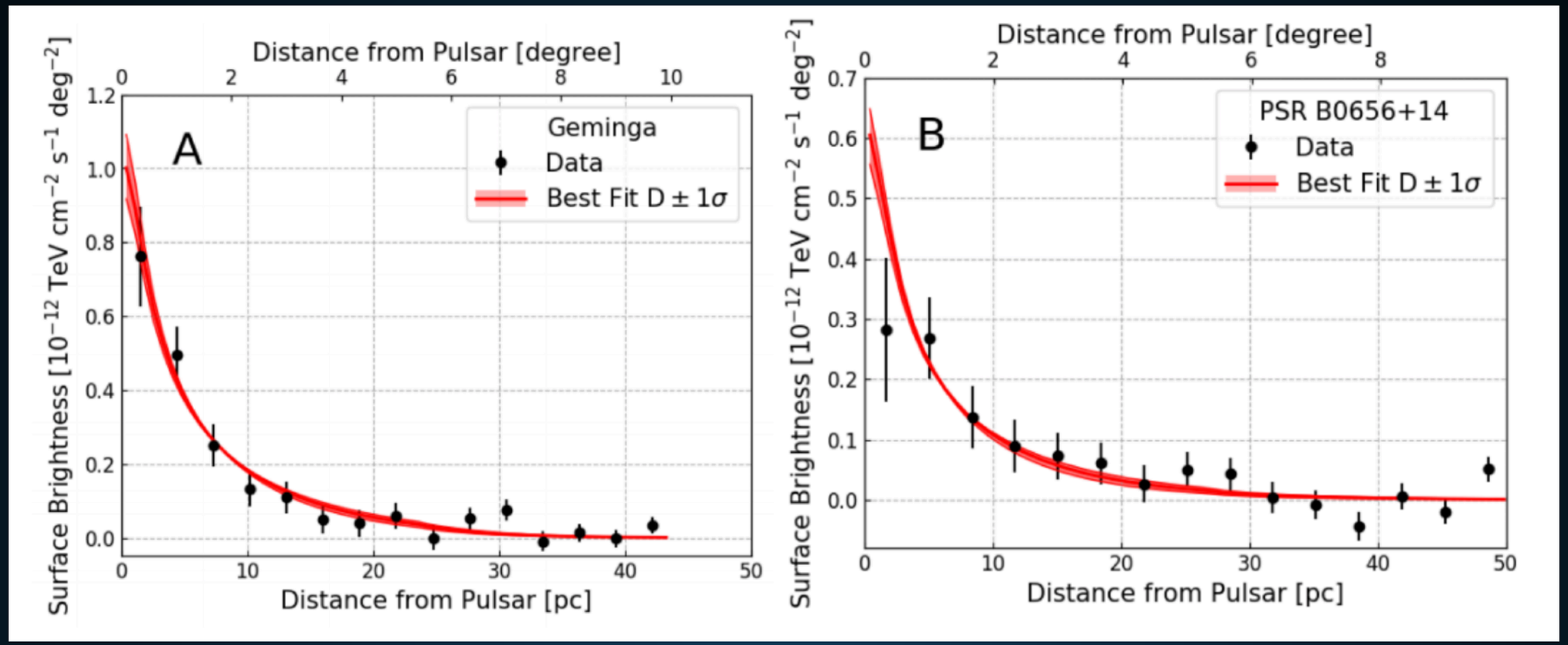

- **Why TeV Halos?**
  - **These sources are <u>much smaller</u> than ISM diffusion**

$$\tau_{loss} \approx 30\ \text{Kyr} \qquad D_0 \approx 5 \times 10^{28}\ \text{cm}^2\,\text{s}^{-1}$$

$$L = \sqrt{Dt} \approx 2000\ \text{pc}$$

TEV HALOS

HAWC Collaboration (Nature; 1711.06223)

Pulsar Parameters		**Geminga**	**PSR B0656+14**
(Right ascension, declination) (J2000 source location)	[degrees]	(98.48, 17.77)	(104.95, 14.24)
τ_c (characteristic age)	[years]	342,000	110,000
T (spin period)	[seconds]	0.237	0.385
d (distance)	[parsecs]	250^{+120}_{-62}	288^{+33}_{-27}
dE/dt (energy loss rate due to pulsar's spin slowing)	[x10^{34} ergs/sec]	3.26	3.8
Model Values			
θ_0 (θ_d for 20 TeV γ-ray)	[degrees]	5.5 ± 0.7	4.8 ± 0.6
N_0	[x10^{-15} photons/TeV/cm^2 /sec]	$13.6^{+2.0}_{-1.7}$	$5.6^{+2.5}_{-1.7}$
α		2.34 ± 0.07	2.14 ± 0.23
D_{100} (Diffusion coefficient of 100TeV electrons from joint fit of two PWNe)	[x10^{27} cm^2/sec]	4.5 ± 1.2	4.5 ± 1.2
D_{100}(Diffusion coefficient of 100TeV electrons from individual fit of PWN)	[x10^{27} cm^2/sec]	$3.2^{+1.4}_{-1.0}$	15^{+49}_{-9}
Energy Range	[TeV]	8 to 40	8 to 40
Luminosity in gamma-rays over this energy range	[x10^{31} erg/sec]	11x(d/250 parsec)^2	4.5x(d/288 parsec)^2
Assumed Parameters			
L_0 (initial spin down power)	[x10^{36} ergs/sec]	27.8	4.0
W_e (total energy released since pulsar's birth)	[x10^{48} ergs]	11.0	1.5

Table 1: Pulsar parameters, values of parameters from the model fitting to the observed extended gamma-ray emission, and assumed parameters of our model. Pulsar parameters are from (14).

HESS OBSERVATIONS

HESS Collaboration (1702.08280)

- **"TeV PWN" observed by HESS have similar fluxes and extensions.**

Table 1 HGPS sources considered as firmly identified pulsar wind nebulae in this paper.

HGPS name	ATNF name	Canonical name	lg $\dot{E}$	τ_c (kyr)	d (kpc)	PSR offset (pc)	Γ	R_{PWN} (pc)	$L_{1-10\,TeV}$ (10^{33} erg s^{-1})
J1813−178[1]	J1813−1749		37.75	5.60	4.70	< 2	2.07 ± 0.05	4.0 ± 0.3	19.0 ± 1.5
J1833−105	J1833−1034	G21.5−0.9[2]	37.53	4.85	4.10	< 2	2.42 ± 0.19	< 4	2.6 ± 0.5
J1514−591	B1509−58	MSH 15−52[3]	37.23	1.56	4.40	< 4	2.26 ± 0.03	11.1 ± 2.0	52.1 ± 1.8
J1930+188	J1930+1852	G54.1+0.3[4]	37.08	2.89	7.00	< 10	2.6 ± 0.3	< 9	5.5 ± 1.8
J1420−607	J1420−6048	Kookaburra (K2)[5]	37.00	13.0	5.61	5.1 ± 1.2	2.20 ± 0.05	7.9 ± 0.6	44 ± 3
J1849−000	J1849−0001	IGR J18490−0000[6]	36.99	42.9	7.00	< 10	1.97 ± 0.09	11.0 ± 1.9	12 ± 2
J1846−029	J1846−0258	Kes 75[2]	36.91	0.728	5.80	< 2	2.41 ± 0.09	< 3	6.0 ± 0.7
J0835−455	B0833−45	Vela X[7]	36.84	11.3	0.280	2.37 ± 0.18	1.89 ± 0.03	2.9 ± 0.3	0.83 ± 0.11*
J1837−069[8]	J1838−0655		36.74	22.7	6.60	17 ± 3	2.54 ± 0.04	41 ± 4	204 ± 8
J1418−609	J1418−6058	Kookaburra (Rabbit)[5]	36.69	10.3	5.00	7.3 ± 1.5	2.26 ± 0.05	9.4 ± 0.9	31 ± 3
J1356−645[9]	J1357−6429		36.49	7.31	2.50	5.5 ± 1.4	2.20 ± 0.08	10.1 ± 0.9	14.7 ± 1.4
J1825−137[10]	B1823−13		36.45	21.4	3.93	33 ± 6	2.38 ± 0.03	32 ± 2	116 ± 4
J1119−614	J1119−6127	G292.2−0.5[11]	36.36	1.61	8.40	< 11	2.64 ± 0.12	14 ± 2	23 ± 4
J1303−631[12]	J1301−6305		36.23	11.0	6.65	20.5 ± 1.8	2.33 ± 0.02	20.6 ± 1.7	96 ± 5

Table 4 Candidate pulsar wind nebulae from the pre-selection.

HGPS name	ATNF name	lg $\dot{E}$	τ_c (kyr)	d (kpc)	PSR offset (pc)	Γ	R_{PWN} (pc)	$L_{1-10\,TeV}$ (10^{33} erg s^{-1})	Rating 1	2	3	4
J1616−508 (1)	J1617−5055	37.20	8.13	6.82	< 26	2.34 ± 0.06	28 ± 4	162 ± 9	★	★	★	★
J1023−575	J1023−5746	37.04	4.60	8.00	< 9	2.36 ± 0.05	23.2 ± 1.2	67 ± 5	★	★	★	★
J1809−193 (1)	J1811−1925	36.81	23.3	5.00	29 ± 7	2.38 ± 0.07	35 ± 4	53 ± 3	★	★	★	↯
J1857+026	J1856+0245	36.66	20.6	9.01	21 ± 6	2.57 ± 0.06	41 ± 9	118 ± 13	★	★	★	★
J1640−465	J1640−4631 (1)	36.64	3.35	12.8	< 20	2.55 ± 0.04	25 ± 8	210 ± 12	★	★	★	★
J1641−462	J1640−4631 (2)	36.64	3.35	12.8	50 ± 5	2.50 ± 0.11	< 14	17 ± 4	↯	⋆	★	⋆
J1708−443	B1706−44	36.53	17.5	2.60	17 ± 3	2.17 ± 0.08	12.7 ± 1.4	6.6 ± 0.9	★	★	★	★
J1908+063	J1907+0602	36.45	19.5	3.21	21 ± 3	2.26 ± 0.06	27.2 ± 1.5	28 ± 2	★	★	★	★
J1018−589A	J1016−5857 (1)	36.41	21.0	8.00	47.5 ± 1.6	2.24 ± 0.13	< 4	8.1 ± 1.4	↯	⋆	★	⋆
J1018−589B	J1016−5857 (2)	36.41	21.0	8.00	25 ± 7	2.20 ± 0.09	21 ± 4	23 ± 5	★	★	★	★
J1804−216	B1800−21	36.34	15.8	4.40	18 ± 5	2.69 ± 0.04	19 ± 3	42.5 ± 2.0	★	★	★	★
J1809−193 (2)	J1809−1917	36.26	51.3	3.55	< 17	2.38 ± 0.07	25 ± 3	26.9 ± 1.5	★	★	★	★
J1616−508 (2)	B1610−50	36.20	7.42	7.94	60 ± 7	2.34 ± 0.06	32 ± 5	220 ± 12	↯	★	★	★
J1718−385	J1718−3825	36.11	89.5	3.60	5.4 ± 1.6	1.77 ± 0.06	7.2 ± 0.9	4.6 ± 0.8	★	★	★	★
J1026−582	J1028−5819	35.92	90.0	2.33	9 ± 2	1.81 ± 0.10	5.3 ± 1.6	1.7 ± 0.5	↯	★	★	★
J1832−085	B1830−08 (1)	35.76	147	4.50	23.3 ± 1.5	2.38 ± 0.14	< 4	1.7 ± 0.4	↯	↯	★	⋆
J1834−087	B1830−08 (2)	35.76	147	4.50	32.3 ± 1.9	2.61 ± 0.07	17 ± 3	25.8 ± 2.0	↯	★	★	↯
J1858+020	J1857+0143	35.65	71.0	5.75	38 ± 3	2.39 ± 0.12	7.9 ± 1.6	7.1 ± 1.5	↯	★	★	↯
J1745−303	B1742−30 (1)	33.93	546	0.200	1.42 ± 0.15	2.57 ± 0.06	0.62 ± 0.07	0.014 ± 0.003	↯	↯	★	↯
J1746−308	B1742−30 (2)	33.93	546	0.200	< 1.1	3.3 ± 0.2	0.56 ± 0.12	0.009 ± 0.003	⋆	↯	★	↯

HESS OBSERVATIONS

HESS Collaboration (1702.08280)

- **There is a significant role for HAWC to play in rigorously determining these extensions (HAWC South for Better Comparisons!)**

Table 1 HGPS sources considered as firmly identified pulsar wind nebulae in this paper.

HGPS name	ATNF name	Canonical name	lg $\dot{E}$	τ_c (kyr)	d (kpc)	PSR offset (pc)	Γ	R_{PWN} (pc)	$L_{1-10\,TeV}$ (10^{33} erg s^{-1})
J1813−178[1]	J1813−1749		37.75	5.60	4.70	< 2	2.07 ± 0.05	4.0 ± 0.3	19.0 ± 1.5
J1833−105	J1833−1034	G21.5−0.9[2]	37.53	4.85	4.10	< 2	2.42 ± 0.19	< 4	2.6 ± 0.5
J1514−591	B1509−58	MSH 15−52[3]	37.23	1.56	4.40	< 4	2.26 ± 0.03	11.1 ± 2.0	52.1 ± 1.8
J1930+188	J1930+1852	G54.1+0.3[4]	37.08	2.89	7.00	< 10	2.6 ± 0.3	< 9	5.5 ± 1.8
J1420−607	J1420−6048	Kookaburra (K2)[5]	37.00	13.0	5.61	5.1 ± 1.2	2.20 ± 0.05	7.9 ± 0.6	44 ± 3
J1849−000	J1849−0001	IGR J18490−0000[6]	36.99	42.9	7.00	< 10	1.97 ± 0.09	11.0 ± 1.9	12 ± 2
J1846−029	J1846−0258	Kes 75[2]	36.91	0.728	5.80	< 2	2.41 ± 0.09	< 3	6.0 ± 0.7
J0835−455	B0833−45	Vela X[7]	36.84	11.3	0.280	2.37 ± 0.18	1.89 ± 0.03	2.9 ± 0.3	0.83 ± 0.11*
J1837−069[8]	J1838−0655		36.74	22.7	6.60	17 ± 3	2.54 ± 0.04	41 ± 4	204 ± 8
J1418−609	J1418−6058	Kookaburra (Rabbit)[5]	36.69	10.3	5.00	7.3 ± 1.5	2.26 ± 0.05	9.4 ± 0.9	31 ± 3
J1356−645[9]	J1357−6429		36.49	7.31	2.50	5.5 ± 1.4	2.20 ± 0.08	10.1 ± 0.9	14.7 ± 1.4
J1825−137[10]	B1823−13		36.45	21.4	3.93	33 ± 6	2.38 ± 0.03	32 ± 2	116 ± 4
J1119−614	J1119−6127	G292.2−0.5[11]	36.36	1.61	8.40	< 11	2.64 ± 0.12	14 ± 2	23 ± 4
J1303−631[12]	J1301−6305		36.23	11.0	6.65	20.5 ± 1.8	2.33 ± 0.02	20.6 ± 1.7	96 ± 5

Table 4 Candidate pulsar wind nebulae from the pre-selection.

HGPS name	ATNF name	lg $\dot{E}$	τ_c (kyr)	d (kpc)	PSR offset (pc)	Γ	R_{PWN} (pc)	$L_{1-10\,TeV}$ (10^{33} erg s^{-1})	Rating 1	2	3	4
J1616−508 (1)	J1617−5055	37.20	8.13	6.82	< 26	2.34 ± 0.06	28 ± 4	162 ± 9	★	★	★	★
J1023−575	J1023−5746	37.04	4.60	8.00	< 9	2.36 ± 0.05	23.2 ± 1.2	67 ± 5	★	★	★	★
J1809−193 (1)	J1811−1925	36.81	23.3	5.00	29 ± 7	2.38 ± 0.07	35 ± 4	53 ± 3	★	★	★	↯
J1857+026	J1856+0245	36.66	20.6	9.01	21 ± 6	2.57 ± 0.06	41 ± 9	118 ± 13	★	★	★	★
J1640−465	J1640−4631 (1)	36.64	3.35	12.8	< 20	2.55 ± 0.04	25 ± 8	210 ± 12	★	★	★	★
J1641−462	J1640−4631 (2)	36.64	3.35	12.8	50 ± 5	2.50 ± 0.11	< 14	17 ± 4	↯	⋆	★	⋆
J1708−443	B1706−44	36.53	17.5	2.60	17 ± 3	2.17 ± 0.08	12.7 ± 1.4	6.6 ± 0.9	★	★	★	★
J1908+063	J1907+0602	36.45	19.5	3.21	21 ± 3	2.26 ± 0.06	27.2 ± 1.5	28 ± 2	★	★	★	★
J1018−589A	J1016−5857 (1)	36.41	21.0	8.00	47.5 ± 1.6	2.24 ± 0.13	< 4	8.1 ± 1.4	↯	⋆	★	⋆
J1018−589B	J1016−5857 (2)	36.41	21.0	8.00	25 ± 7	2.20 ± 0.09	21 ± 4	23 ± 5	★	★	★	★
J1804−216	B1800−21	36.34	15.8	4.40	18 ± 5	2.69 ± 0.04	19 ± 3	42.5 ± 2.0	★	★	★	★
J1809−193 (2)	J1809−1917	36.26	51.3	3.55	< 17	2.38 ± 0.07	25 ± 3	26.9 ± 1.5	★	★	★	★
J1616−508 (2)	B1610−50	36.20	7.42	7.94	60 ± 7	2.34 ± 0.06	32 ± 5	220 ± 12	↯	★	★	★
J1718−385	J1718−3825	36.11	89.5	3.60	5.4 ± 1.6	1.77 ± 0.06	7.2 ± 0.9	4.6 ± 0.8	★	★	★	★
J1026−582	J1028−5819	35.92	90.0	2.33	9 ± 2	1.81 ± 0.10	5.3 ± 1.6	1.7 ± 0.5	↯	★	★	★
J1832−085	B1830−08 (1)	35.76	147	4.50	23.3 ± 1.5	2.38 ± 0.14	< 4	1.7 ± 0.4	↯	↯	★	⋆
J1834−087	B1830−08 (2)	35.76	147	4.50	32.3 ± 1.9	2.61 ± 0.07	17 ± 3	25.8 ± 2.0	↯	★	★	↯
J1858+020	J1857+0143	35.65	71.0	5.75	38 ± 3	2.39 ± 0.12	7.9 ± 1.6	7.1 ± 1.5	↯	★	★	↯
J1745−303	B1742−30 (1)	33.93	546	0.200	1.42 ± 0.15	2.57 ± 0.06	0.62 ± 0.07	0.014 ± 0.003	↯	↯	★	↯
J1746−308	B1742−30 (2)	33.93	546	0.200	< 1.1	3.3 ± 0.2	0.56 ± 0.12	0.009 ± 0.003	⋆	↯	★	↯

EMISSION FROM PULSARS WILL DOMINATE THE NEXT DECADE OF TEV ASTRONOMY

THE GLOBAL POPULATION OF TEV HALOS

- Extrapolate to the full population.

- The following correlation is consistent with the data.

$$\phi_{\text{TeV halo}} = \left(\frac{\dot{E}_{\text{psr}}}{\dot{E}_{\text{Geminga}}}\right)\left(\frac{d^2_{\text{Geminga}}}{d^2_{\text{psr}}}\right)\phi_{\text{Geminga}}$$

- This is also consistent with our theoretical model, where the pulsar serves as the only power source.

- Note: Using Monogem would increases fluxes by nearly a factor of 2. The power law of this correlation doesn't greatly affect the results.

HAWC OBSERVATIONS OF TEV HALO LUMINOSITIES Linden et al. (PRD; 1703.09704)

ATNF Name	Dec. (°)	Distance (kpc)	Age (kyr)	Spindown Lum. (erg s^{-1})	Spindown Flux (erg s^{-1} kpc^{-2})	2HWC
J0633+1746	17.77	0.25	342	3.2e34	4.1e34	2HWC J0631+169
B0656+14	14.23	0.29	111	3.8e34	3.6e34	2HWC J0700+143
B1951+32	32.87	3.00	107	3.7e36	3.3e34	—
J1740+1000	10.00	1.23	114	2.3e35	1.2e34	—
J1913+1011	10.18	4.61	169	2.9e36	1.1e34	2HWC J1912+099
J1831-0952	-9.86	3.68	128	1.1e36	6.4e33	2HWC J1831-098
J2032+4127	41.45	1.70	181	1.7e35	4.7e33	2HWC J2031+415
B1822-09	-9.58	0.30	232	4.6e33	4.1e33	—
B1830-08	-8.45	4.50	147	5.8e35	2.3e33	—
J1913+0904	9.07	3.00	147	1.6e35	1.4e33	—
B0540+23	23.48	1.56	253	4.1e34	1.4e33	**2HWC J0543+233**

- Can produce a ranked list of the 57 ATNF pulsars in the HAWC field of view.
- 5 of the brightest 7 have been detected.

HAWC detection of TeV emission near PSR B0540+23

ATel #10941; *Colas Riviere (University of Maryland), Henrike Fleischhack (Michigan Technological University), Andres Sandoval (Universidad Nacional Autonoma de Mexico) on behalf of the HAWC collaboration*
on 9 Nov 2017; 23:11 UT
Credential Certification: Colas Riviere (riviere@umd.edu)

Subjects: Gamma Ray, TeV, VHE, Pulsar

Tweet Recommend 5

The High Altitude Water Cherenkov (HAWC) collaboration reports the discovery of a new TeV gamma-ray source HAWC J0543+233. It was discovered in a search for extended sources of radius 0.5° in a dataset of 911 days (ranging from November 2014 to August 2017) with a test statistic value of 36 (6σ pre-trials), following the method presented in Abeysekara et al. 2017, ApJ, 843, 40. The measured J2000.0 equatorial position is RA=85.78°, Dec=23.40° with a statistical uncertainty of 0.2°. HAWC J0543+233 was close to passing the selection criteria of the 2HWC catalog (Abeysekara et al. 2017, ApJ, 843, 40, see HAWC J0543+233 in 2HWC map), which it now fulfills with the additional data.
HAWC J0543+233 is positionally coincident with the pulsar PSR B0540+23 (Edot = 4.1e+34 erg s-1, dist = 1.56 kpc, age = 253 kyr). It is the third low Edot, middle-aged pulsar announced to be detected with a TeV halo, along with Geminga and B0656+14. It was predicted to be one of the next such detection by HAWC by Linden et al., 2017, arXiv:1703.09704.
Using a simple source model consisting of a disk of radius 0.5°, the measured spectral index is -2.3 ± 0.2 and the differential flux at 7 TeV is (7.9 ± 2.3) × 10^-15 TeV-1 cm-2 s-1. The errors are statistical only. Further morphological and spectral analysis as well as studies of the systematic uncertainty are ongoing.

TEV HALOS ARE A GENERIC FEATURE OF PULSARS

- **5 / 39 sources in the 2HWC catalog are correlated with bright, middle-aged (100 – 400 kyr) pulsars.**

2HWC Name	ATNF Name	Distance (kpc)	Angular Separation	Projected Separation	Expected Flux ($\times 10^{-15}$)	Actual Flux ($\times 10^{-15}$)	Flux Ratio	Expected Extension	Actual Extension	Age (kyr)	Chance Overlap
J0700+143	B0656+14	0.29	0.18°	0.91 pc	43.0	23.0	1.87	2.0°	1.73°	111	0.0
J0631+169	J0633+1746	0.25	0.89°	3.88 pc	48.7	48.7	1.0	2.0°	2.0°	342	0.0
J1912+099	J1913+1011	4.61	0.34°	27.36 pc	13.0	36.6	0.36	0.11°	0.7°	169	0.30
J2031+415	J2032+4127	1.70	0.11°	3.26 pc	5.59	61.6	0.091	0.29°	0.7°	181	0.002
J1831-098	J1831-0952	3.68	0.04°	2.57 pc	7.70	95.8	0.080	0.14°	0.9°	128	0.006

- **12 others with young pulsars**
  - **2.3 chance overlaps**
  - **TeV emission may be contaminated by SNR**

2HWC Name	ATNF Name	Distance (kpc)	Angular Separation	Projected Separation	Expected Flux ($\times 10^{-15}$)	Actual Flux ($\times 10^{-15}$)	Flux Ratio	Expected Extension	Actual Extension	Age (kyr)	Chance Overlap
J1930+188	J1930+1852	7.0	0.03°	3.67 pc	23.2	9.8	2.37	0.07°	0.0°	2.89	0.002
J1814-173	J1813-1749	4.7	0.54°	44.30 pc	243	152	1.60	0.11°	1.0°	5.6	0.61
J2019+367	J2021+3651	1.8	0.27°	8.48 pc	99.8	58.2	1.71	0.28°	0.7°	17.2	0.04
J1928+177	J1928+1746	4.34	0.03°	2.27 pc	8.08	10.0	0.81	0.11°	0.0°	82.6	0.002
J1908+063	J1907+0602	2.58	0.36°	16.21 pc	40.0	85.0	0.47	0.2°	0.8°	19.5	0.26
J2020+403	J2021+4026	2.15	0.18°	6.75 pc	2.48	18.5	0.134	0.23°	0.0°	77	0.01
J1857+027	J1856+0245	6.32	0.12°	13.24 pc	11.0	97.0	0.11	0.08°	0.9°	20.6	0.06
J1825-134	J1826-1334	3.61	0.20°	12.66 pc	20.5	249	0.082	0.14°	0.9°	21.4	0.14
J1837-065	J1838-0655	6.60	0.38°	43.77 pc	12.0	341	0.035	0.08°	2.0°	22.7	0.48
J1837-065	J1837-0604	4.78	0.50°	41.71 pc	8.3	341	0.024	0.10°	2.0°	33.8	0.68
J2006+341	J2004+3429	10.8	0.42°	80.07 pc	0.48	24.5	0.019	0.04°	0.9°	18.5	0.08

Tauris & Manchester (1998)

- Tauris and Manchester (1998) calculated the beaming angle from a population of young and middle-aged pulsars.

$$f = \left[1.1 \left(\log_{10}\left(\frac{\tau}{100\ \mathrm{Myr}}\right)\right)^2 + 15\right]\ \%$$

- This varies between 15-30%.

- 1/f pulsars are unseen in radio surveys.

MISSING TEV HALOS

Linden et al. (PRD; 1703.09704)

2HWC Name	ATNF Name	Distance (kpc)	Angular Separation	Projected Separation	Expected Flux ($\times 10^{-15}$)	Actual Flux ($\times 10^{-15}$)	Flux Ratio	Expected Extension	Actual Extension	Age (kyr)	Chance Overlap
J0700+143	B0656+14	0.29	0.18°	0.91 pc	43.0	23.0	1.87	2.0°	1.73°	111	0.0
J0631+169	J0633+1746	0.25	0.89°	3.88 pc	48.7	48.7	1.0	2.0°	2.0°	342	0.0
J1912+099	J1913+1011	4.61	0.34°	27.36 pc	13.0	36.6	0.36	0.11°	0.7°	169	0.30
J2031+415	J2032+4127	1.70	0.11°	3.26 pc	5.59	61.6	0.091	0.29°	0.7°	181	0.002
J1831-098	J1831-0952	3.68	0.04°	2.57 pc	7.70	95.8	0.080	0.14°	0.9°	128	0.006

2HWC Name	ATNF Name	Distance (kpc)	Angular Separation	Projected Separation	Expected Flux ($\times 10^{-15}$)	Actual Flux ($\times 10^{-15}$)	Flux Ratio	Expected Extension	Actual Extension	Age (kyr)	Chance Overlap
J1930+188	J1930+1852	7.0	0.03°	3.67 pc	23.2	9.8	2.37	0.07°	0.0°	2.89	0.002
J1814-173	J1813-1749	4.7	0.54°	44.30 pc	243	152	1.60	0.11°	1.0°	5.6	0.61
J2019+367	J2021+3651	1.8	0.27°	8.48 pc	99.8	58.2	1.71	0.28°	0.7°	17.2	0.04
J1928+177	J1928+1746	4.34	0.03°	2.27 pc	8.08	10.0	0.81	0.11°	0.0°	82.6	0.002
J1908+063	J1907+0602	2.58	0.36°	16.21 pc	40.0	85.0	0.47	0.2°	0.8°	19.5	0.26
J2020+403	J2021+4026	2.15	0.18°	6.75 pc	2.48	18.5	0.134	0.23°	0.0°	77	0.01
J1857+027	J1856+0245	6.32	0.12°	13.24 pc	11.0	97.0	0.11	0.08°	0.9°	20.6	0.06
J1825-134	J1826-1334	3.61	0.20°	12.66 pc	20.5	249	0.082	0.14°	0.9°	21.4	0.14
J1837-065	J1838-0655	6.60	0.38°	43.77 pc	12.0	341	0.035	0.08°	2.0°	22.7	0.48
J1837-065	J1837-0604	4.78	0.50°	41.71 pc	8.3	341	0.024	0.10°	2.0°	33.8	0.68
J2006+341	J2004+3429	10.8	0.42°	80.07 pc	0.48	24.5	0.019	0.04°	0.9°	18.5	0.08

- Correcting for the beaming fraction implies that 56^{+15}_{-11} TeV halos are currently observed by HAWC.
- However, only 39 HAWC sources total.
- Chance overlaps, SNR contamination must be taken into account.

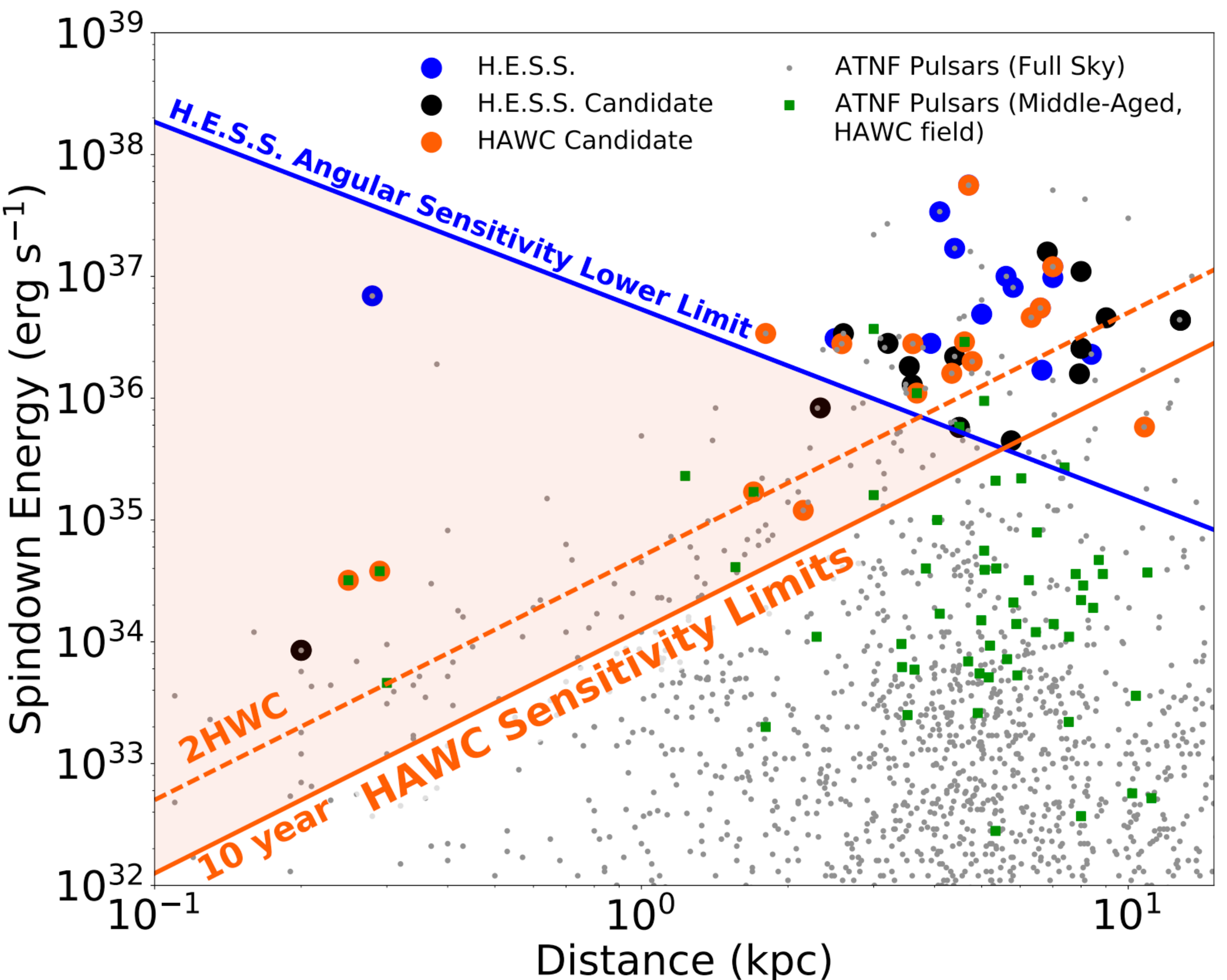
H.E.S.S.
H.E.S.S. Candidate
HAWC Candidate
ATNF Pulsars (Full Sky)
ATNF Pulsars (Middle-Aged, HAWC field)
H.E.S.S. Angular Sensitivity Lower Limit
2HWC
10 year HAWC Sensitivity Limits
Spindown Energy (erg s^{-1})
Distance (kpc)
10^{39}
10^{38}
10^{37}
10^{36}
10^{35}
10^{34}
10^{33}
10^{32}
10^{-1}
10^{0}
10^{1}

TEV HALOS SURROUNDING MSPS

Hooper & Linden (1803.08046)

- Unknown if MSPs follow the same correlation.

- Some indication that this would be possible:
  - Geminga is an isolated pulsar, with a spin-down energy that is not significantly larger than some MSPs.
  - Some MSPs have similar PWN activity.

- Brightest MSPs slightly too dim to be detected.

Hooper & Linden (1803.08046)

- Use the 2HWC Survey Public Tool.

- Get TS values of each MSP, and look for a distribution of high-TS values.

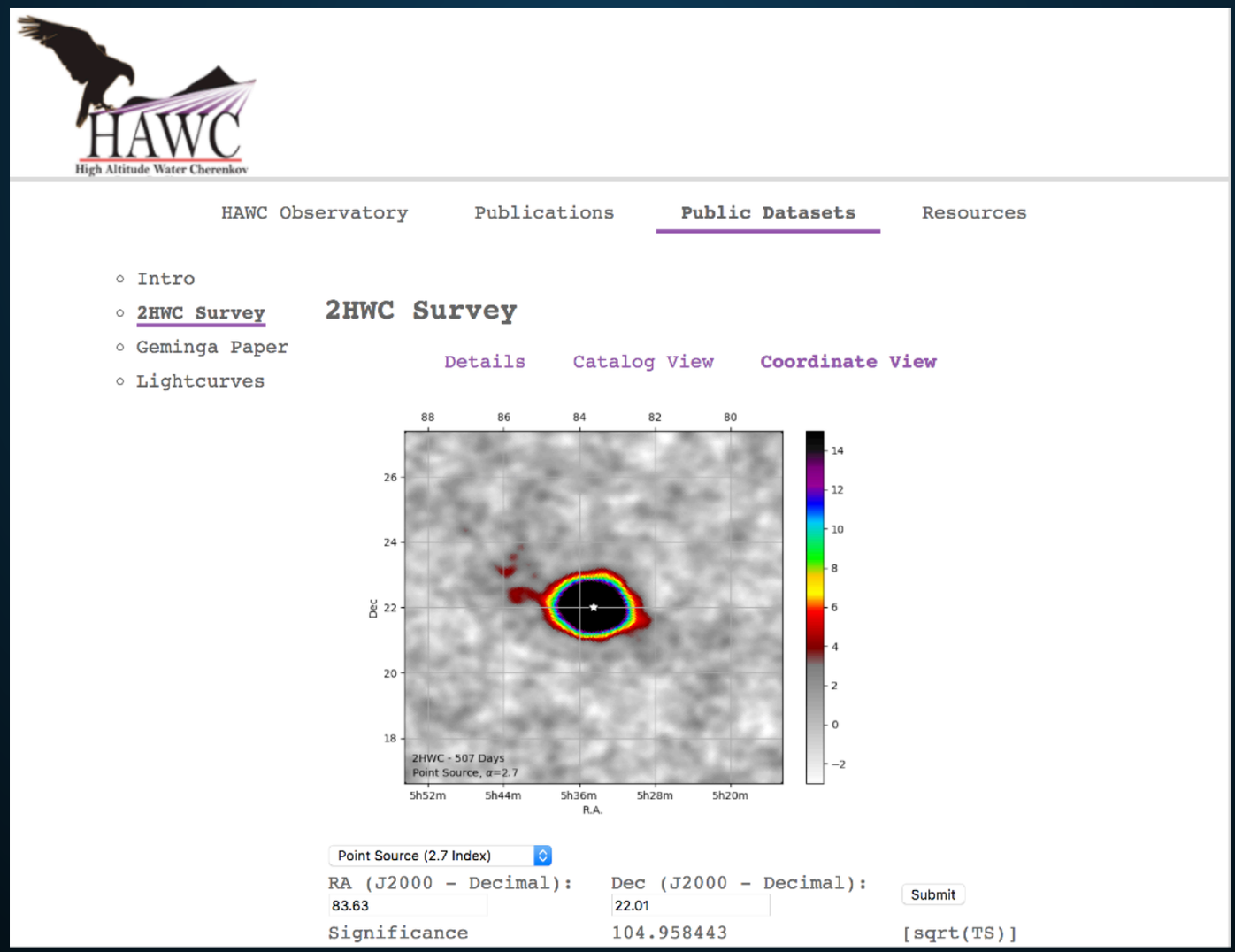

TEV HALOS SURROUNDING MSPS

Hooper & Linden (1803.08046)

PSR Name	$\dot{E}$ (erg/s)	Distance (kpc)	$\dot{E}/D^2$ erg/kpc^2/s	Method	$(\mathrm{TS})^{1/2}$ (point-like)	$(\mathrm{TS})^{1/2}$ (Geminga-like)
J1400-1431	9.7×10^{33}	0.28	1.2×10^{35}	DM [6]	-1.17	-1.65
J0034-0534	3.0×10^{34}	0.54 ± 0.10	$1.0^{+0.5}_{-0.3} \times 10^{35}$	DM [16]	1.40	0.40
J1737-0811	4.3×10^{33}	0.21	9.8×10^{34}	DM [6]	1.57	-0.985
J1231-1411	1.8×10^{34}	0.44 ± 0.05	$9.3^{+2.5}_{-1.8} \times 10^{34}$	DM [17]	-0.52	-1.33
J2214+3000	1.9×10^{34}	$0.59^{+0.66}_{-0.21}$	$5.5^{+7.7}_{-4.2} \times 10^{34}$	P [18]	-0.31	0.09
J1023+0038	9.8×10^{34}	$1.37^{+0.04}_{-0.03}$	$5.2^{+0.3}_{-0.3} \times 10^{34}$	P [19]	**2.18**	1.63
J0030+0451	3.5×10^{33}	$0.28^{+0.10}_{-0.06}$	$4.5^{+2.8}_{-2.0} \times 10^{34}$	P [20]	-0.48	**2.07**
J1843-1113	6.0×10^{34}	1.26	3.8×10^{34}	DM [6]	0.16	0.49
J1643-1224	7.4×10^{33}	$0.45^{+0.11}_{-0.07}$	$3.7^{+1.5}_{-1.3} \times 10^{34}$	P [21]	-0.45	0.73
J0023+0923	1.6×10^{34}	$0.69^{+0.21}_{-0.11}$	$3.4^{+1.4}_{-1.4} \times 10^{34}$	DM [22]	0.83	0.07
J1300+1240	1.9×10^{34}	$0.77^{+0.34}_{-0.18}$	$3.2^{+2.3}_{-1.7} \times 10^{34}$	P [23]	-0.26	0.68
J1744-1134	5.2×10^{33}	$0.42^{+0.03}_{-0.02}$	$3.0^{+0.3}_{-0.2} \times 10^{34}$	P [21]	0.13	-0.79
J1959+2048	1.6×10^{35}	$2.49^{+0.16}_{-0.49}$	$2.6^{+1.4}_{-3.0} \times 10^{34}$	DM [24]	**2.54**	**2.54**
J0337+1715	3.4×10^{34}	1.30	2.0×10^{34}	DM [6]	1.11	1.82
J1741+1351	2.3×10^{34}	$1.08^{+0.04}_{-0.05}$	$2.0^{+0.2}_{-0.1} \times 10^{34}$	P [25]	-0.47	-0.13
J2017+0603	1.4×10^{34}	$0.83^{+0.60}_{-0.24}$	$1.9^{+1.8}_{-1.3} \times 10^{34}$	DM [18]	-0.02	0.92
J2339-0533	2.3×10^{34}	1.10	1.9×10^{34}	DM [6]	-1.35	-2.07
J1939+2134	1.1×10^{36}	$7.7^{+7.7}_{-2.6}$	$1.9^{+2.3}_{-1.4} \times 10^{34}$	P [21]	**2.61**	**2.61**
J0613-0200	1.3×10^{34}	$0.90^{+0.40}_{-0.20}$	$1.6^{+1.0}_{-0.8} \times 10^{34}$	P [20]	1.02	**2.34**
J1719-1438	1.6×10^{33}	0.34	1.4×10^{34}	DM [6]	0.27	-0.44
J1911-1114	1.2×10^{34}	1.07	1.0×10^{34}	DM [6]	-0.48	-0.76
J1745-0952	5.0×10^{32}	0.23	9.5×10^{33}	DM [6]	-1.40	-2.29
J0218+4232	2.4×10^{35}	$6.3^{+8.0}_{-1.7}$	$6.1^{+8.9}_{-5.0} \times 10^{33}$	P [26]	0.36	0.36
J0557+1550	1.7×10^{34}	1.83	5.1×10^{33}	DM [6]	-0.20	-0.34

- Select 24 ATNF MSPs with highest E/d² fluxes.
- Listed in order here, along with observed TS values.
- Probability of observing 4 systems above 2.07 is 3.2σ, assuming Normal Statistics.

TEV HALOS SURROUNDING MSPS

Hooper & Linden (1803.08046)

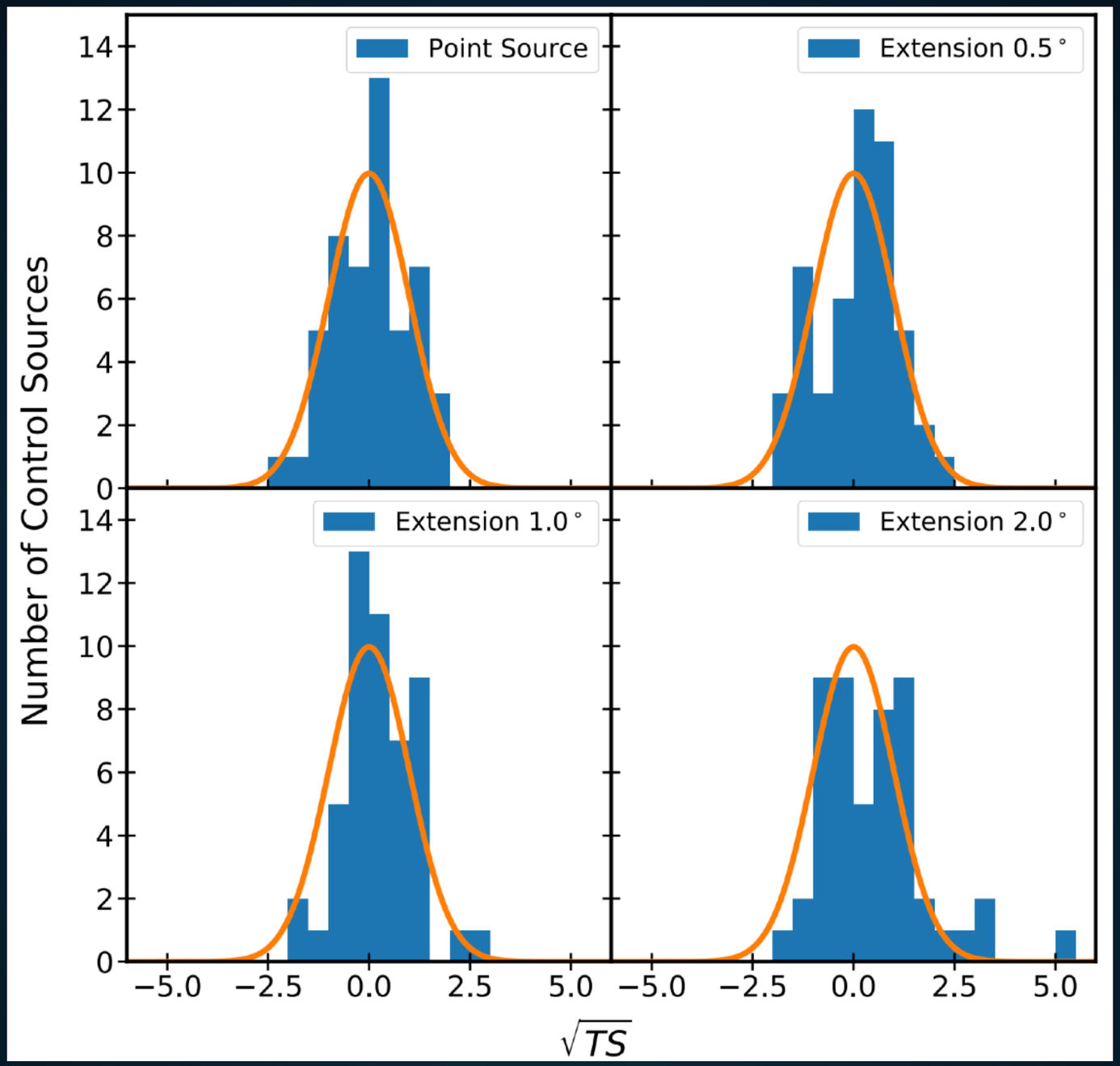

- Need to develop an appropriate distribution of background sources.
- Pick the 50 dimmest MSPs in the sample. Normal approximation appears good, except for 2° extension, which appears to include larger fluctuations.

ADDITIONAL IMPLICATIONS FOR MSPS

Hooper & Linden (1803.08046)

- Unknown if MSPs follow the same correlation.

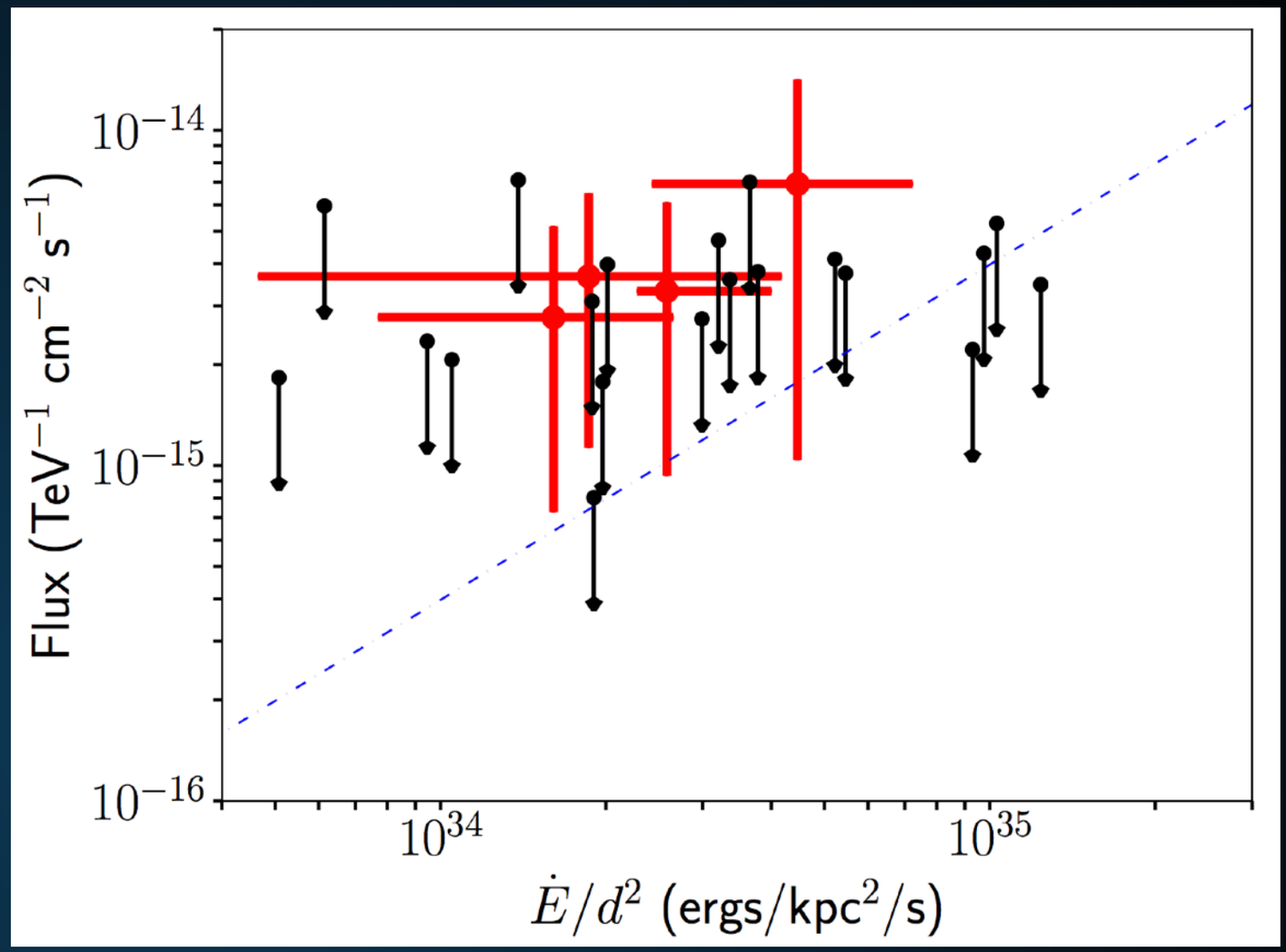

- Even brightest MSPs slightly too dim to be individually detected.

- Stacking a population of 24 MSPs provides moderate (~3σ) evidence that MSPs also produce TeV halos, further increasing the population.

ADDITIONAL IMPLICATIONS FOR MSPS

Hooper & Linden (1803.08046)

- This study can be drastically improved:
  - Full likelihood stacking instead of simple TS.
  - Distribution of spectral and spatial extensions.
  - Dispersion in Geminga-like model.
  - Uncertainties in distance measurements.
- Results indicate that in a few years HAWC can definitively test MSP models.
- Young Pulsars Too!

IMPLICATIONS

IMPLICATION I: THE TEV EXCESS

Linden & Buckman (PRL; 1707.01905)

- **Milagro detects bright diffuse TeV emission along the Galactic plane.**

- **Difficult to explain with pion decay, due to steeply falling local hadronic CR spectrum.**

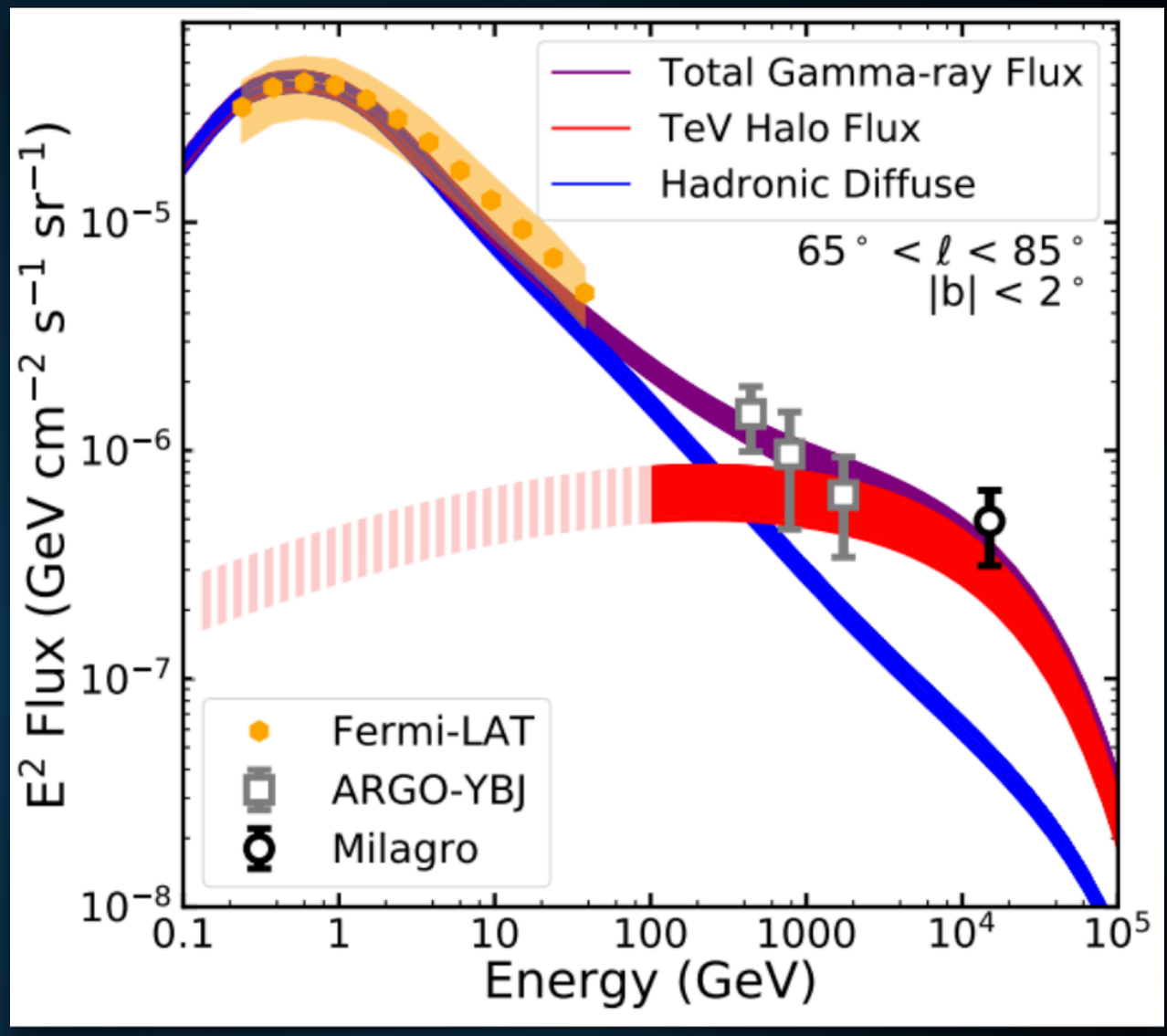

- **The Geminga and Monogem TeV halo spectra naturally explain both the spectrum and intensity of this emission.**

IMPLICATION II: THE GALACTIC CENTER PEVATRON

Hooper, Cholis, TL (1603.07730)
HESS Collaboration (1603.07730)

- HESS observes ~50 TeV diffuse emission from the Galactic center.
- If this is hadronic, it is evidence for PeV proton acceleration.
- TeV halos from Geminga and Monogem explain the spectrum and intensity of this emission.

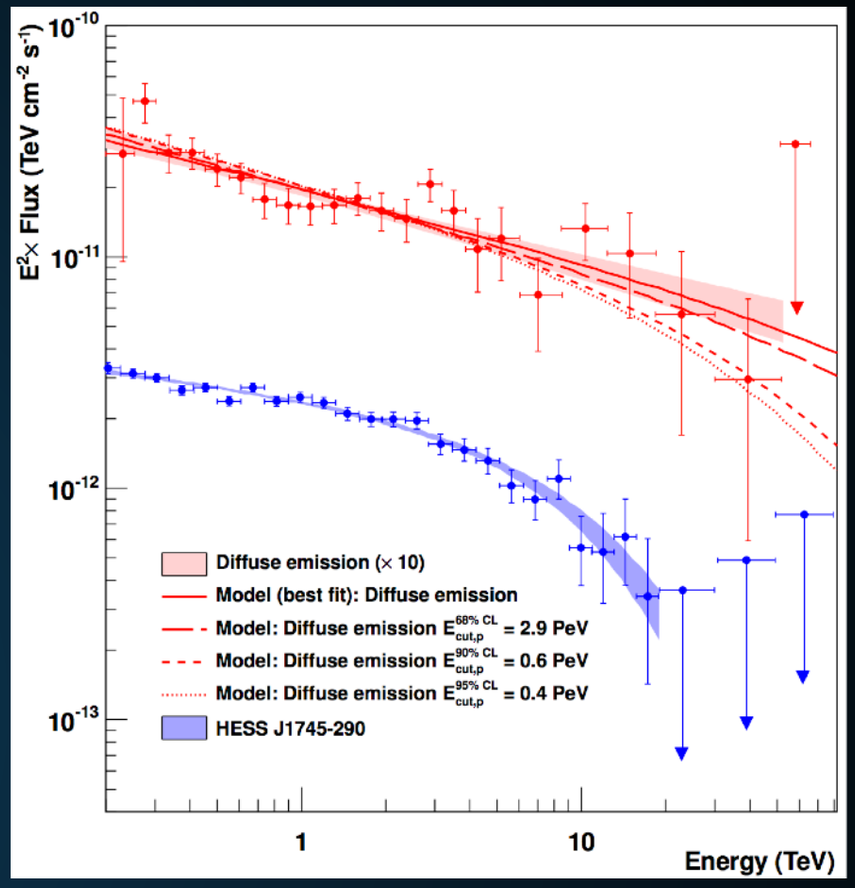

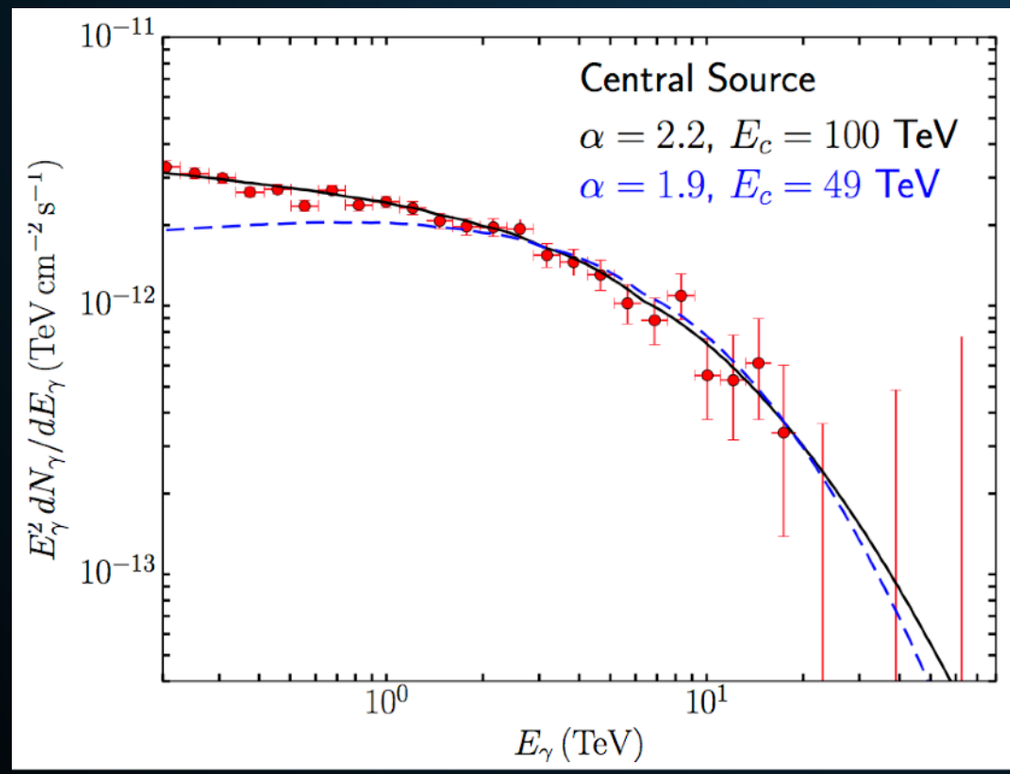

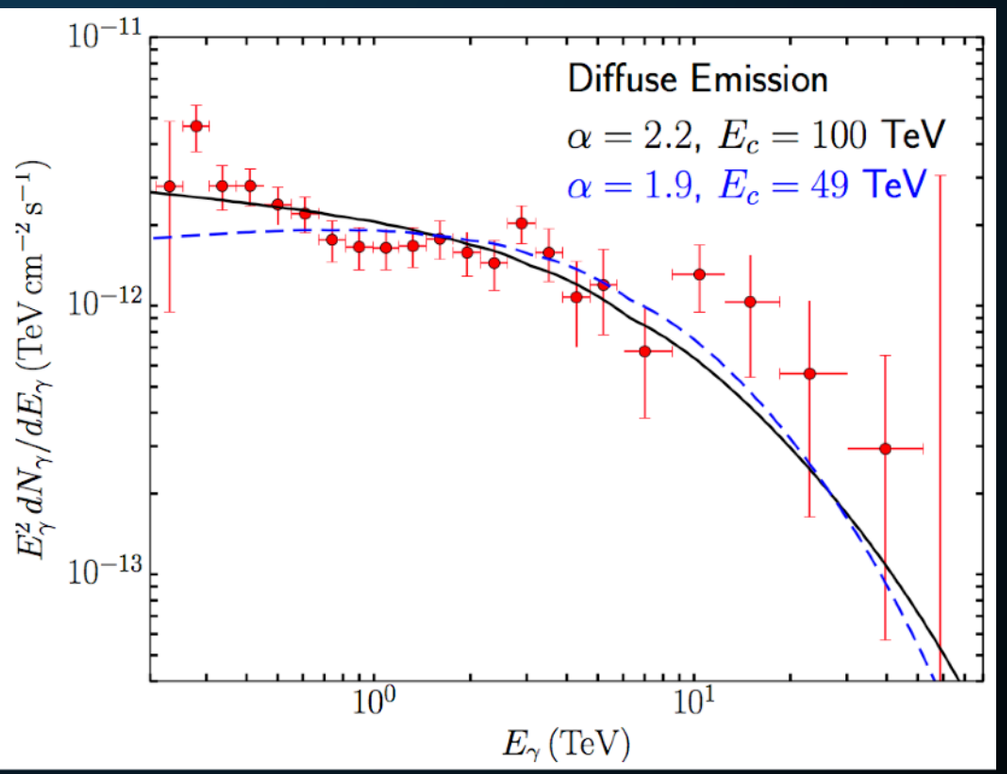

IMPLICATION III: THE POSITRON EXCESS

HAWC Collaboration (Nature; 1711.06223)

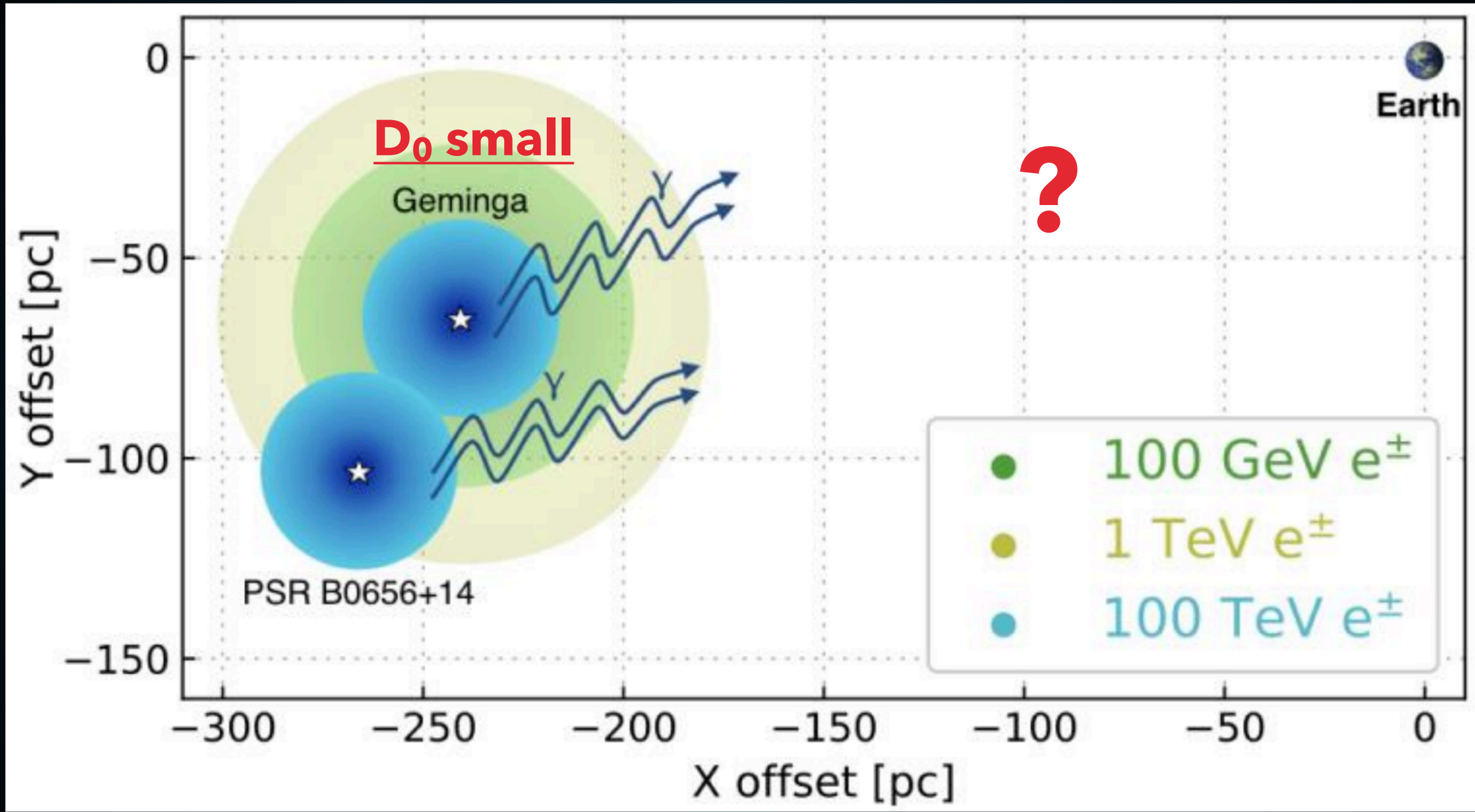

Two Zone Model: First electrons escape from halo

$$\tau_{diff} \propto \frac{L^2}{D_0 E^\delta} \qquad \tau_{loss} \propto E^{-1}$$

$$\left(\frac{\Delta E}{E}\right) \propto \frac{\tau_{diff}}{\tau_{loss}} \propto E^{1-\delta} L^2$$

- Low-energy electrons lose energy slower, lose less energy before exiting the TeV halo.
- If 10 TeV electrons lose 90% of their energy, 100 GeV electrons lose 10% of their energy.

TWO POSSIBLE ASSUMPTIONS

HAWC Collaboration (1711.06223)

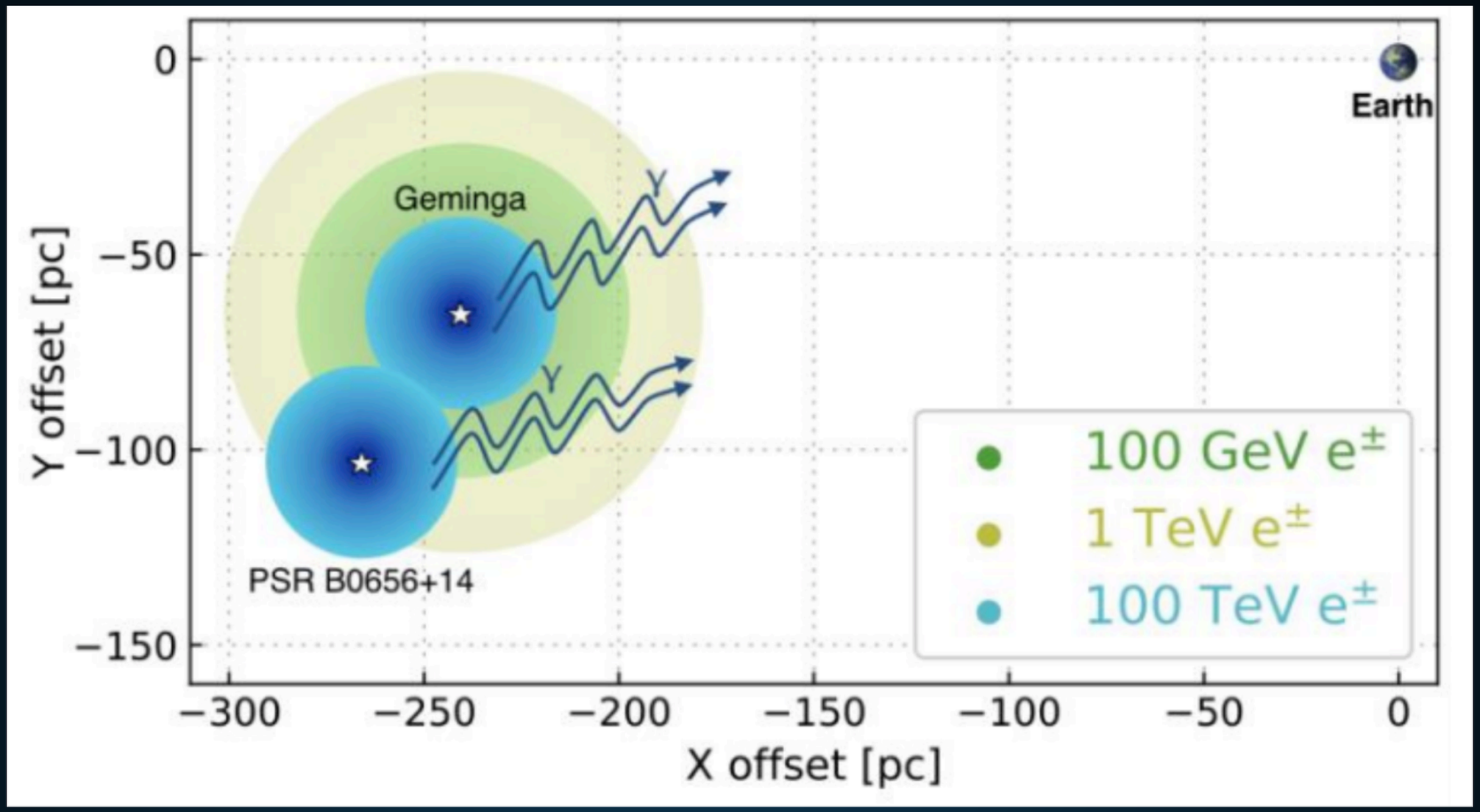

- **<u>Assumption 1:</u> The diffusion constant measured near Geminga and Monogem stands as the first measurement of the diffusion constant near Earth**

TWO POSSIBLE ASSUMPTIONS

HAWC Collaboration (1711.06223)

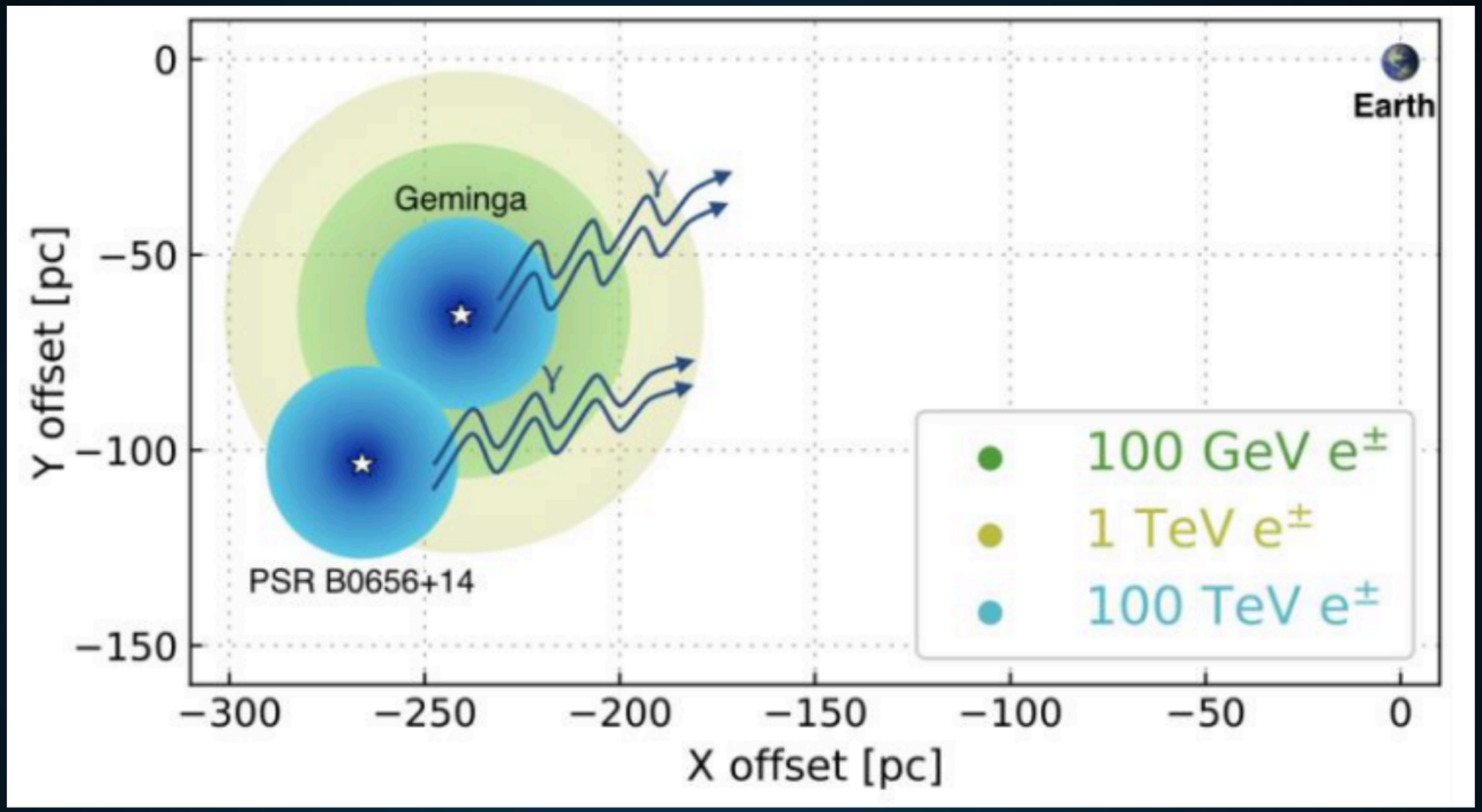

- **Methodology:** Apply the low ($D_0 \sim 1 \times 10^{26}$ cm^2 s^{-1}) diffusion constant for the full positron journey.

TWO POSSIBLE ASSUMPTIONS

$$\tau_{diff} \propto \frac{L^2}{D_0 E^{\delta}} \qquad \tau_{loss} \propto E^{-1}$$

$$L(E) \propto \sqrt{D_0 E^{\delta - 1}}$$

- <u>Implication:</u> Assuming Kolmogorov Diffusion ($\delta = 0.33$), 100 GeV e^+e^- propagate about 4.5x as far.

TWO POSSIBLE ASSUMPTIONS

$L(10\ \text{TeV}) = 20\ \text{pc}$

$L(100\ \text{GeV}) = 92\ \text{pc}$

- <u>Implication:</u> Assuming Kolmogorov Diffusion ($\delta = 0.33$), 100 GeV electrons propagate about 4.5x as far.
- Earth is ~250 pc away

TWO POSSIBLE ASSUMPTIONS

HAWC Collaboration (1711.06223)

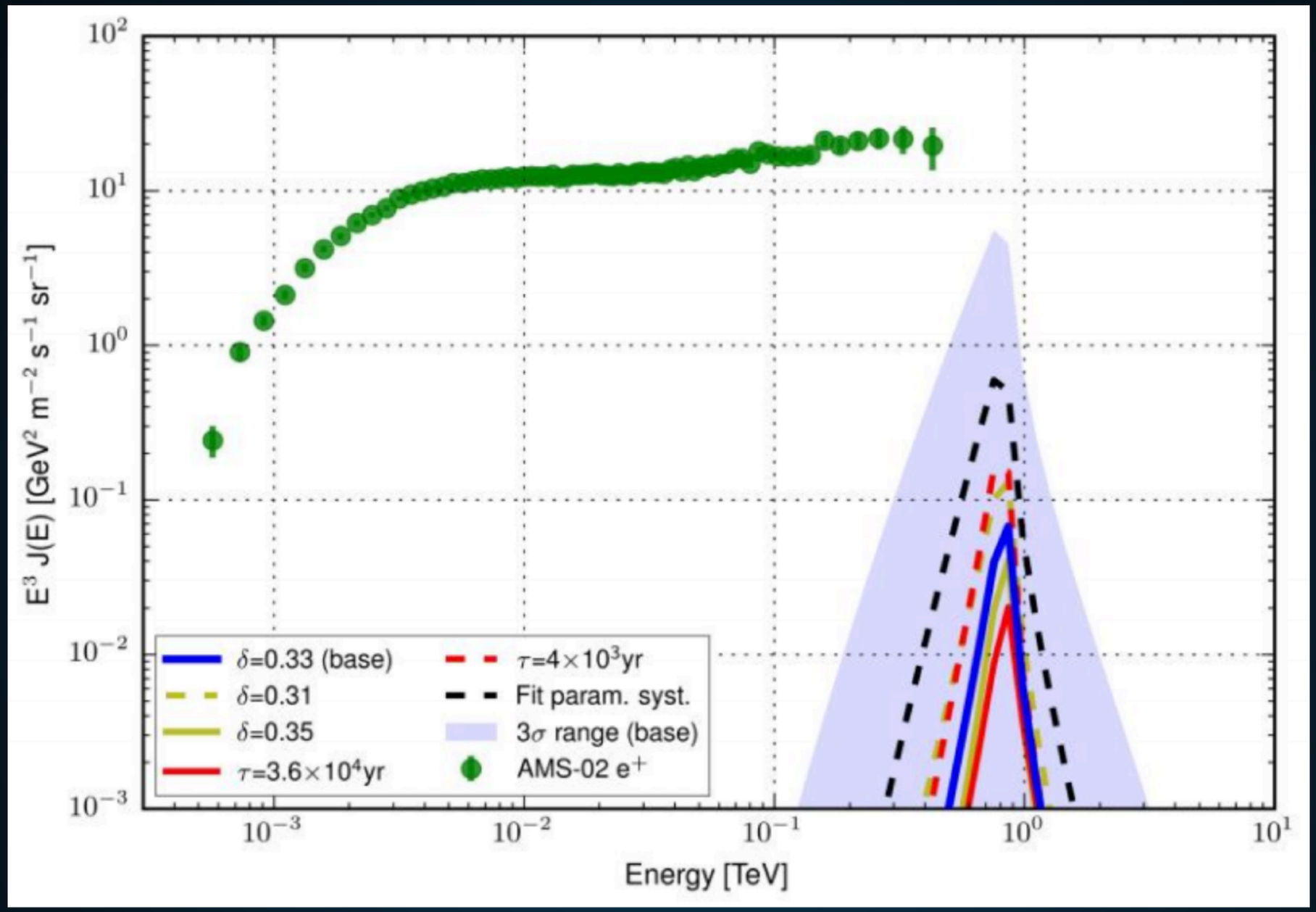

- **Implication:** **Geminga and Monogem do not explain the positron excess.**

TWO POSSIBLE ASSUMPTIONS

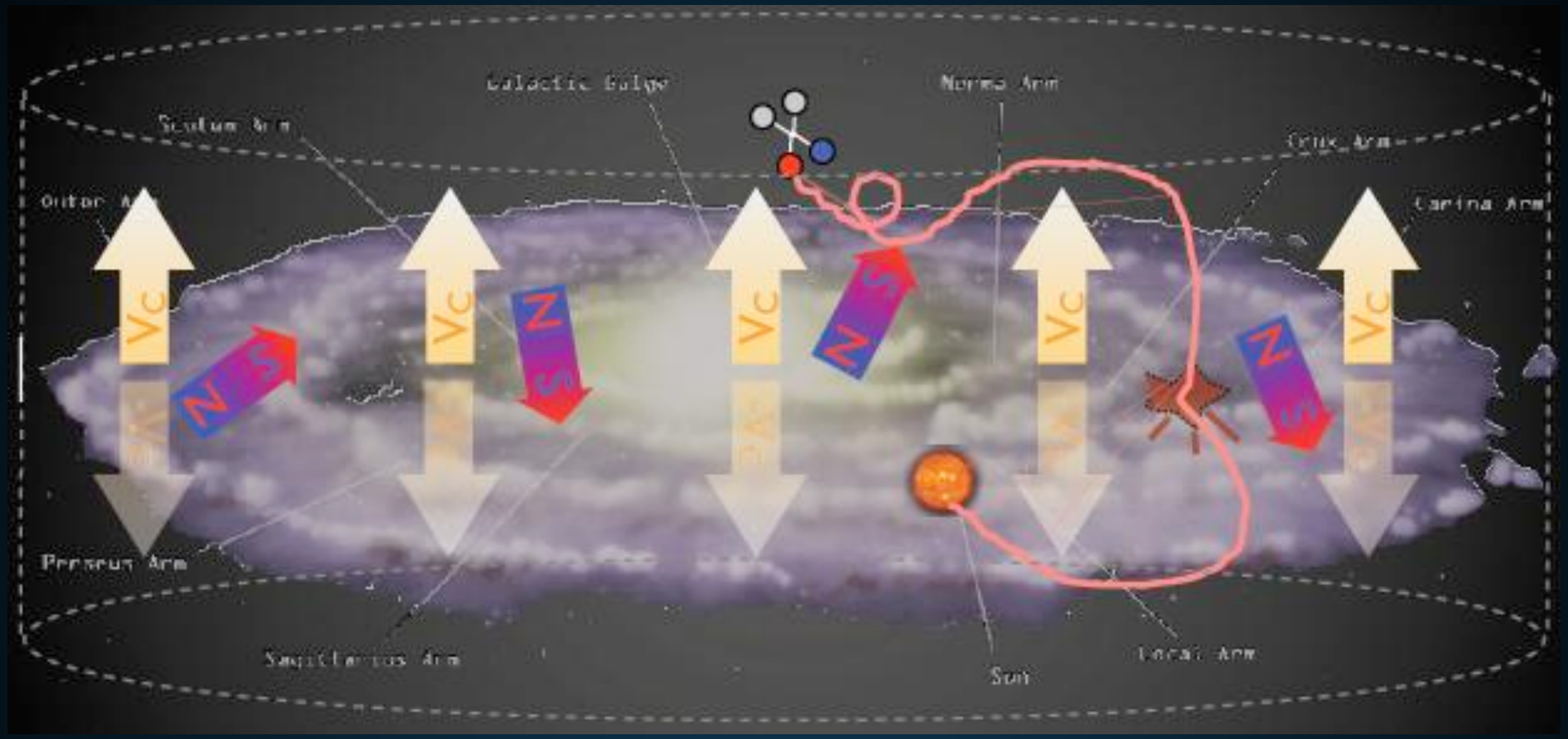

- <u>Assumption 2:</u> **Measurements of cosmic-ray primary to secondary ratios (e.g. by AMS-02) imply that the local diffusion constant is high. The diffusion constant near Geminga and Monogem is local to those sources.**

WHAT HAPPENS TO THE LOW-ENERGY E^+E^-? Hooper et al. (1702.08436)

Two Zone Model: First electrons escape from halo

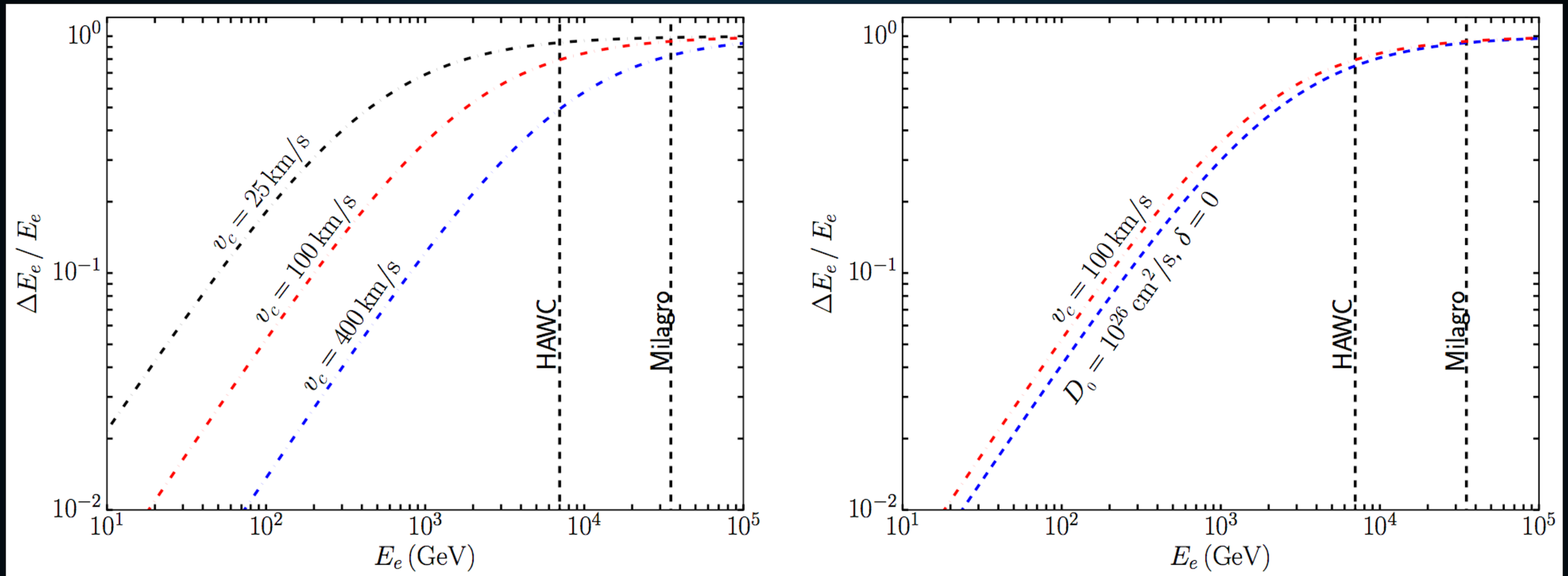

- Low-energy electrons lose energy slower, lose less energy before exiting the TeV halo.
- If 10 TeV electrons lose 90% of their energy, 100 GeV electrons lose 10% of their energy.

Two Zone Model: Then electrons propagate through ISM

ELECTRON DIFFUSION NEAR TEV HALOS 1702.08436

- The energy loss timescale in the ISM (5 μG; 1 eV cm^{-3}) is approximately:

$$\tau_{\rm loss} \approx 2 \times 10^4 \ {\rm yr} \left(\frac{10 \ {\rm TeV}}{E_e}\right)$$

- For ISM Diffusion ($D_0 = 5 \times 10^{28}$ cm^{2}s^{-1} δ=0.33), this implies a radial extent of ~250 pc.

- 20 pc extent indicates $D_0 \sim 1 \times 10^{26}$ cm^2 s^{-1}

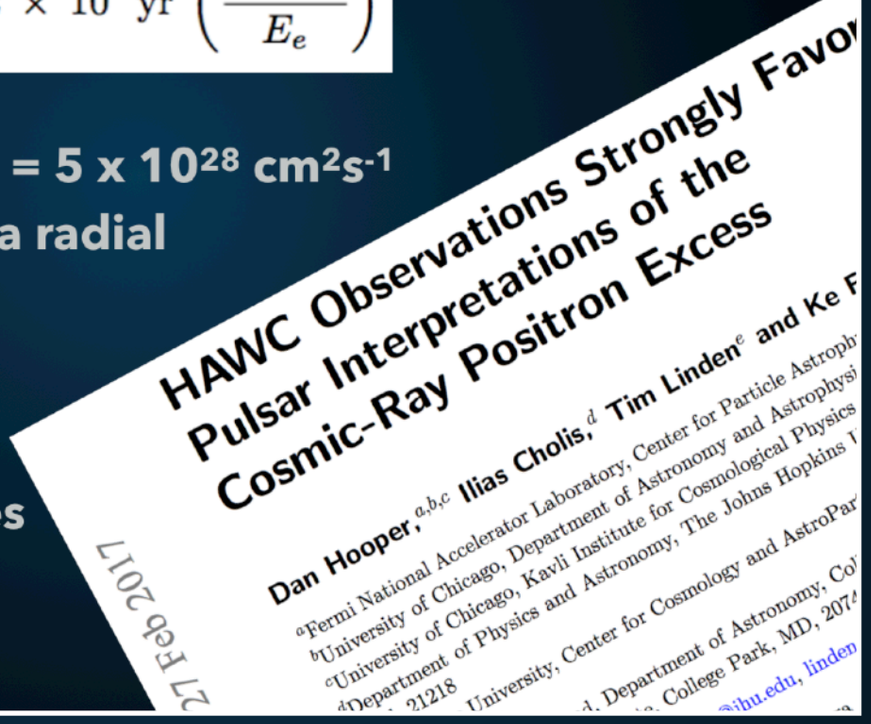

- Outside the TeV halo, diffusion is 500x more efficient.

Two Zone Model: Then electrons propagate through ISM

$$\tau_{diff} \propto \frac{L^2}{D_0 E^{\delta}} \qquad \tau_{loss} \propto E^{-1}$$

$$L(E) \propto \sqrt{D_0 E^{\delta-1}}$$

- Instead of 100 GeV electrons propagating ~90 pc, they now propagate 2000 pc.

TWO POSSIBLE ASSUMPTIONS

Hooper et al. (1702.08436)

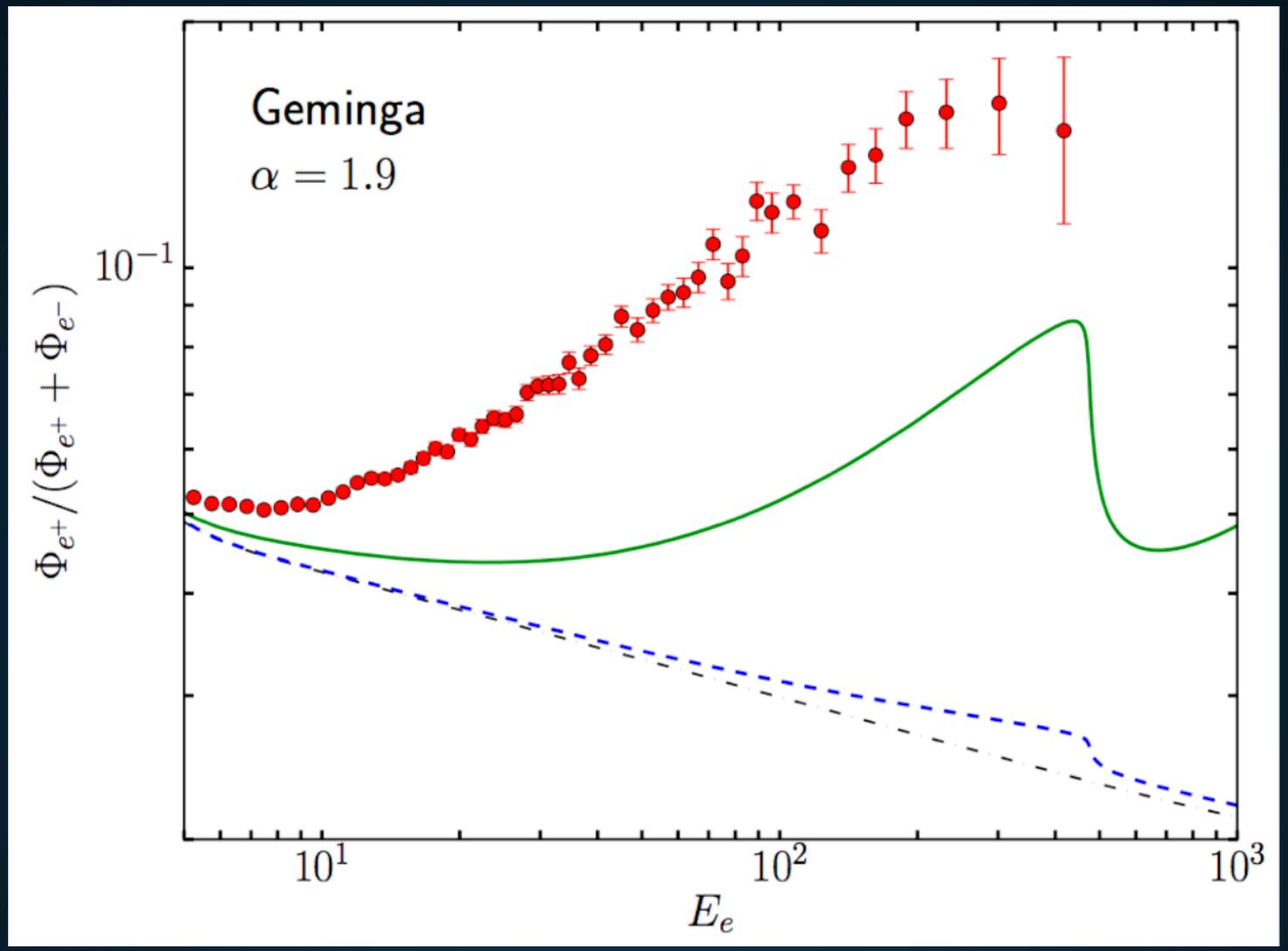

- **Implication:** Low energy positrons make it to Earth and explain the positron excess.

NEW OBSERVATIONS FROM HESS

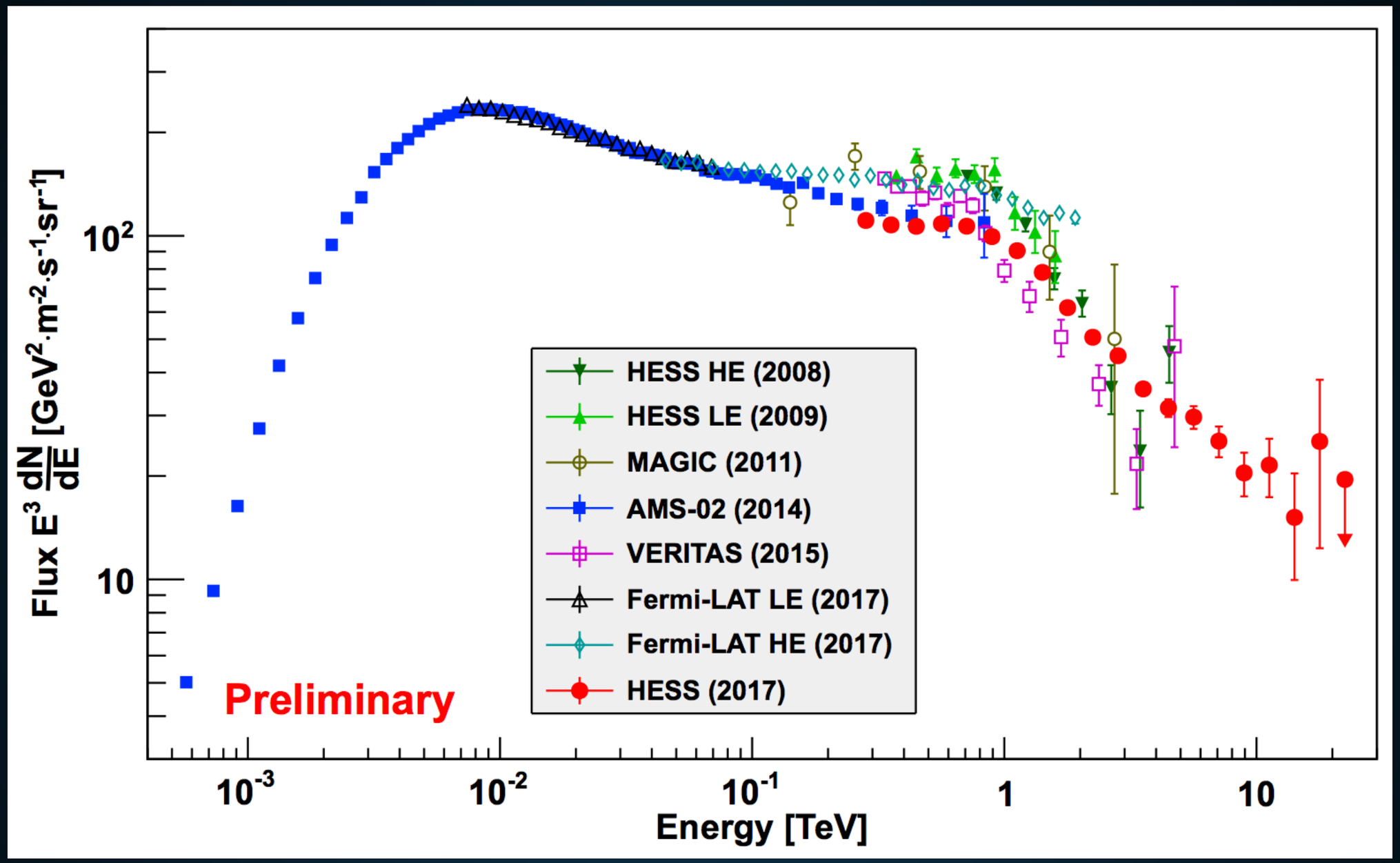

- **Recent H.E.S.S. observations have extended the observed $e^+ + e^-$ spectrum to energies exceeding 20 TeV.**

https://indico.snu.ac.kr/indico/event/15/session/5/contribution/694/material/slides/0.pdf

WHAT HAPPENS TO THE LOW-ENERGY E^+E^-?

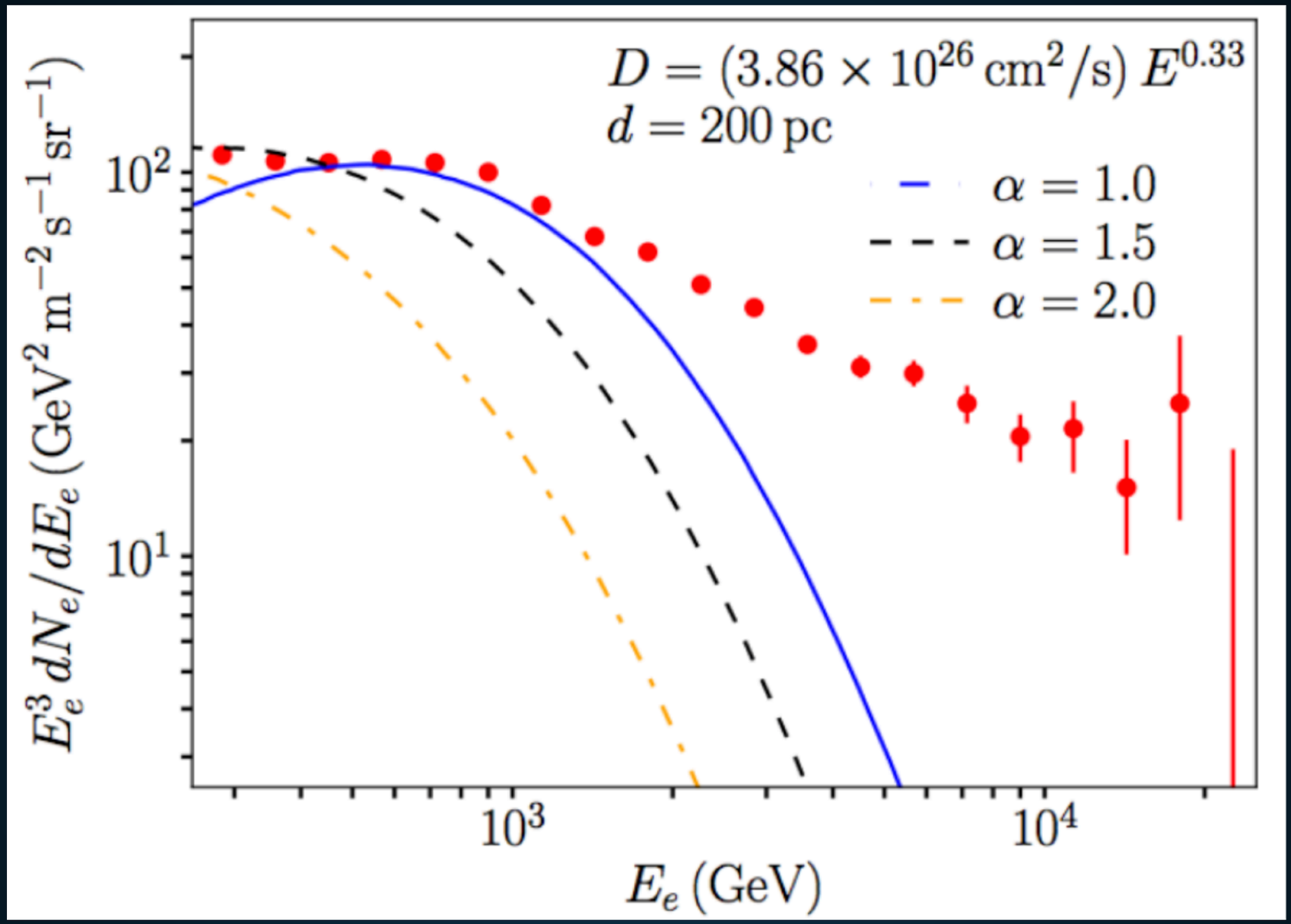

- <u>Assumption 1:</u> **If diffusion constant near Earth is low, any source explaining the electron flux must be within ~30 pc of Earth.**

WHAT HAPPENS TO THE LOW-ENERGY E^+E^-?

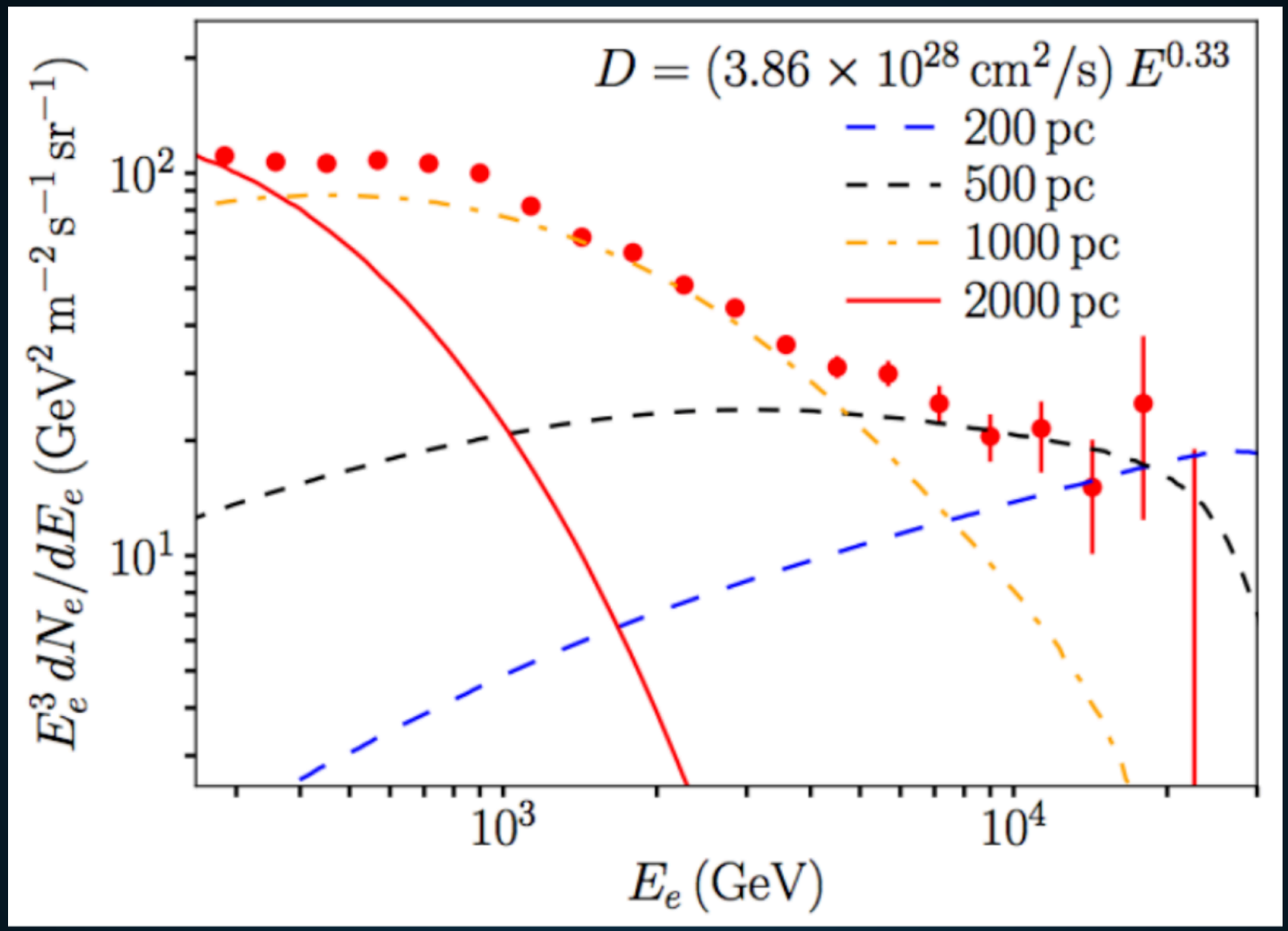

- **<u>Assumption 2:</u> If diffusion is high, the nearest 10 TeV source can be ~500 pc away.**

GC Pulsar Population

Low Energy Electrons Escape

Pulsars Explain Pevatron

Pulsars Explain Positron Excess

Most TeV sources are TeV halos

High Energy Electrons Trapped

TeV halos explain the TeV excess.

Pulsar Population & Energetics

CONCLUSIONS (1/2)

- **TeV halos are a new dynamical object.**

- **Have already observed ~20 objects; >100 inevitable**

- **Simple extrapolations of observed systems imply:**
  - **TeV halos dominate the TeV source number.**
  - **TeV halos dominate Milky Way diffuse emission.**
  - **TeV halos produce the positron excess.**

CONCLUSIONS (2/2)

- **TeV Halos will provide new insight into pulsar birth, death, and evolution, providing a new handle into the multi-wavelength study of neutron star dynamics.**

- **TeV halos provide the first evidence for significant inhomogeneities in Galactic cosmic-ray propagation — new insights into cosmic-ray observations (e.g. AMS-02).**

WHAT IS A TEV HALO?

D'Angelo et al. (1710.10937)

- No current models for the low-diffusion constant within TeV halos.

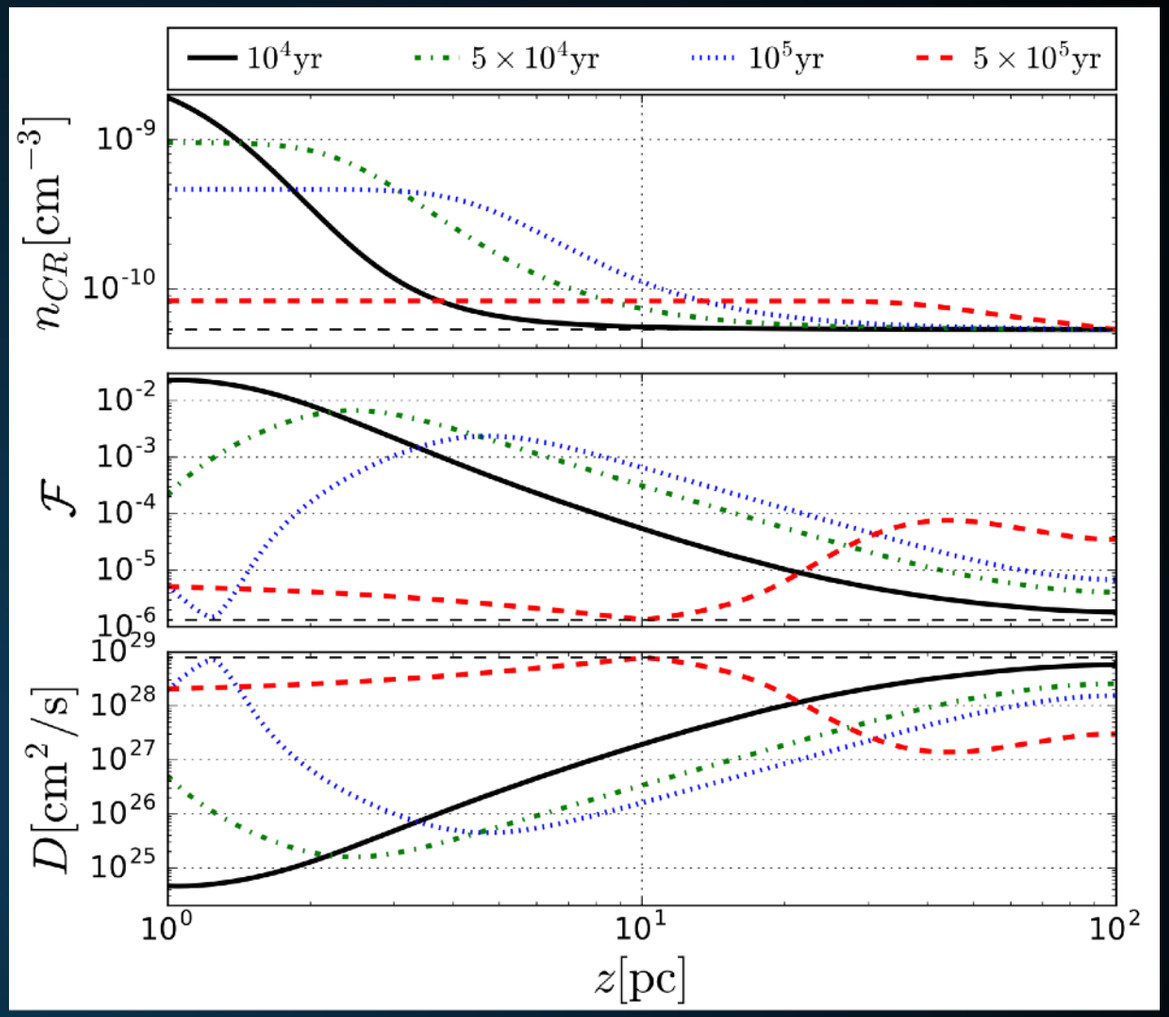

- Can take some evidence from supernova, which can potentially produce regions with inhibited diffusion due to the steep cosmic-ray gradients produced in the SNe.
- Two Options:
  - 1.) Supernova Produces Low-Diffusion around pulsar
    - But Geminga is far from SNR.
  - 2.) Pulsars can produce similar cosmic-ray gradients and inhibit diffusion.

LATITUDE DISTRIBUTION FOR MSPS AND CONTROL SAMPLE